PROJECT REPORT

G.C. LUKEY, J.S.J. VAN DEVENTER, J.L. PROVIS, P. DUXSON

DEPARTMENT OF CHEMICAL AND BIOMOLECULAR ENGINEERING
UNIVERSITY OF MELBOURNE
AUSTRALIA

PROJECT AOARD 054025
DESIGN OF GEOPOLYMERIC MATERIALS BASED ON NANOSTRUCTURAL CHARACTERIZATION AND MODELING
APRIL 2006

Report Documentation Page

Form Approved
OMB No. 0704-0188

1. REPORT DATE	2. REPORT TYPE	3. DATES COVERED
27 JUL 2006	**Final Report (Technical)**	**24-01-2005 to 17-07-2006**

4. TITLE AND SUBTITLE	5a. CONTRACT NUMBER
Design of geopolymeric materials based on nanostructural characterization and modeling	**FA520905P0154**
	5b. GRANT NUMBER
	5c. PROGRAM ELEMENT NUMBER
6. AUTHOR(S) **Grant Lukey**	5d. PROJECT NUMBER
	5e. TASK NUMBER
	5f. WORK UNIT NUMBER
7. PERFORMING ORGANIZATION NAME(S) AND ADDRESS(ES) **University of Melbourne,Department of Chemical Engineering,Melbourne 3010,Australia,AU,3010**	8. PERFORMING ORGANIZATION REPORT NUMBER **AOARD-054025**
9. SPONSORING/MONITORING AGENCY NAME(S) AND ADDRESS(ES) **The US Resarch Labolatory, AOARD/AFOSR, Unit 45002, APO, AP, 96337-5002**	10. SPONSOR/MONITOR'S ACRONYM(S) **AOARD/AFOSR**
	11. SPONSOR/MONITOR'S REPORT NUMBER(S) **AOARD-054025**

12. DISTRIBUTION/AVAILABILITY STATEMENT
Approved for public release; distribution unlimited

13. SUPPLEMENTARY NOTES

14. ABSTRACT

Geopolymers, a class of largely X-ray amorphous aluminosilicate binder materials, have been studied extensively over the past several decades, but largely from an empirical standpoint. The primary aim of this investigation has been to apply a more science-based approach to the study of geopolymers, including introducing a variety of mathematical modelling techniques to the field. Si/Al ordering within the tetrahedral aluminosilicate gel framework is described by a statistical thermodynamic model, which provides an accurate representation of the distribution of Si and Al sites within the framework as well as physically reasonable values for the energy penalty for ordering violation. Direct measurement of the kinetics of the early stages of geopolymeric setting (up to 3 hours) is shown to be possible by energy-dispersive X-ray diffractometry (EDXRD), utilising a high-intensity synchrotron X-ray source to conduct experiments in transmission geometry. Quantification of the results obtained by this technique provides a comparison between the setting rates of different geopolymer-forming systems, and shows clear trends with regard to temperature and Si/Al ratio as well as the nature of the alkali cation (or cation mixture) present. Finally, formulation of a reaction kinetic model for geopolymerisation draws together the results of the project. Based on an existing model for aluminosilicate weathering in aggressive media, the model includes description of dissolution, reorientation and reprecipitation processes including an autocatalytic polycondensation step, and can describe reactions involving either fly ash or metakaolin. Flexible stoichiometry of all polymerised species allows for variations in Si/Al ratios, and the effects of different alkali cations are also described. Model results are compared to calorimetric and EDXRD data, and predictions are consistent with the processes that have previously been postulated to occur during the early stages of geopolymerisation.

15. SUBJECT TERMS

Ceramics, Composite Materials, Polymer Chemistry

16. SECURITY CLASSIFICATION OF:			17. LIMITATION OF ABSTRACT	18. NUMBER OF PAGES	19a. NAME OF RESPONSIBLE PERSON
a. REPORT	b. ABSTRACT	c. THIS PAGE			
unclassified	**unclassified**	**unclassified**		**66**	

ABSTRACT

Geopolymers, a class of largely X-ray amorphous aluminosilicate binder materials, have been studied extensively over the past several decades, but largely from an empirical standpoint. The primary aim of this investigation has been to apply a more science-based approach to the study of geopolymers, including introducing a variety of mathematical modelling techniques to the field. The results described in this report are a combination of work funded by the AOARD proposal as well as

Si/Al ordering within the tetrahedral aluminosilicate gel framework is described by a statistical thermodynamic model, which provides an accurate representation of the distribution of Si and Al sites within the framework as well as physically reasonable values for the energy penalty for ordering violation. Direct measurement of the kinetics of the early stages of geopolymeric setting (up to 3 hours) is shown to be possible by energy-dispersive X-ray diffractometry (EDXRD), utilising a high-intensity synchrotron X-ray source to conduct experiments in transmission geometry. Quantification of the results obtained by this technique provides a comparison between the setting rates of different geopolymer-forming systems, and shows clear trends with regard to temperature and Si/Al ratio as well as the nature of the alkali cation (or cation mixture) present.

Finally, formulation of a reaction kinetic model for geopolymerisation draws together the results of the project. Based on an existing model for aluminosilicate weathering in aggressive media, the model includes description of dissolution, reorientation and reprecipitation processes including an autocatalytic polycondensation step, and can describe reactions involving either fly ash or metakaolin. Flexible stoichiometry of all polymerised species allows for variations in Si/Al ratios, and the effects of different alkali cations are also described. Model results are compared to calorimetric and EDXRD data, and predictions are consistent with the processes that have previously been postulated to occur during the early stages of geopolymerisation.

1. INTRODUCTION TO GEOPOLYMERS

A full review of the literature of geopolymers and the importance of crystallinity in determining geopolymer structure and performance was recently published by Provis *et al.* (2005c). Key results are repeated here in brief.

1.1 FUNDAMENTALS OF GEOPOLYMERIZATION

Commercial and industrial utilisation of alkali-activated aluminosilicate cements, known as 'geopolymers,' has become increasingly widespread over the past several decades as the search for high-performance and/or environmentally sustainable alternatives to ordinary Portland Cement intensifies (Davidovits 1991). However, the underlying mechanisms controlling geopolymer formation, and alkali-activation in general, are currently not well understood (Roy 1999). Development of geopolymer technology has historically been applications-driven rather than technology-driven, meaning that a full understanding of mechanistic processes has not been developed. However, for complete maturation and therefore acceptance of geopolymer technology, further investigation of the mechanisms underlying geopolymerisation is essential.

'Geopolymer' is the name that since the late 1970s has been applied to a wide range of alkaline- or alkali-silicate-activated aluminosilicate binders of composition $M_2O.mAl_2O_3.nSiO_2$, usually with $m \approx 1$ and $2 \leq n \leq 6$, and where M represents one or more alkali metals. Some geopolymers also contain alkaline earth cations, particularly Ca^{2+} in products based on industrial wastes such as granulated blast furnace slag or fly ash, although the question of whether the alkaline earth cations are actually incorporated into the geopolymer structure to a significant extent remains unanswered to date.

Geopolymers may be synthesised at ambient or elevated temperature by alkaline activation of aluminosilicates obtained from industrial wastes, calcined clays, melt-quenched aluminosilicates, natural minerals, or mixtures of two or more of these materials. Activation is achieved by addition of highly concentrated alkali metal hydroxide or silicate solutions. Filler materials including conventional concrete aggregates such as basalt may be used to enhance desired properties including strength and density. However, structural characterisation of both waste-

based materials and the geopolymers synthesised from these materials is greatly complicated by the highly impure nature of these systems, and the use of natural minerals or melt-quenched materials in geopolymerisation is not yet widespread. Composites consisting of a fibre matrix and a geopolymeric binder phase have also been shown to have interesting and potentially very useful properties. Geopolymer-calcium phosphate composites are also being investigated for potential application as a biocompatible synthetic bone replacement material. The primary focus of this project was the formation of geopolymers by alkali metal hydroxide or silicate activation of calcined clays, particularly calcined kaolinite clay (metakaolin). Alkali activation of metakaolin is a convenient 'model system' whereby the behaviour of the more commercially interesting waste-based systems may be understood more fully, as well as having some technological potential in itself.

Geopolymers have created significant interest as high-temperature materials due to their outstanding thermal stability and ability to be used both as a binder in carbon-fibre composites, and also as an additive in epoxy-based systems. The long-term chemical durability of geopolymers has generated significant interest in the field of toxic and nuclear waste immobilisation. However, much analysis remains to be undertaken prior to widespread utilisation, particularly in the highly sensitive area of radioactive waste mitigation, as the consequences of material failure in such an application are extremely serious. Lacking the means to carry out laboratory testing over the geological timescales for which such wastes must be immobilised, the role of mathematical modelling in enabling the use of geopolymers becomes a central one, allowing these materials and their behaviour, both short- and long-term, to be more fully understood from a fundamental level.

Geopolymerisation is a complex multiphase process, involving a series of dissolution-reorientation-solidification reactions analogous to those observed in zeolite synthesis by hydrothermal treatment of solid precursors. Of particular interest to researchers has been the synthesis of low-calcium cements by geopolymerisation of fly ash or metakaolin, providing very strong and durable products.

The geopolymeric binder phase is often described as 'X-ray amorphous' (Palomo and Glasser 1992; Barbosa *et al.* 2000). Many authors have noted formation of phases described as either semicrystalline or polycrystalline, particularly in products synthesised at relatively higher temperature. However, the physicochemical nature of these phases has rarely been subjected to

detailed analysis, and is very difficult to determine due to the complex and intergrown nature of the binder phases and the presence of significant quantities of unreacted raw materials.

The proposed amorphous geopolymer structure is often categorised as an aluminosilicate gel. It has therefore been proposed that this structure is related to the aluminosilicate precursor gels from which zeolites are hydrothermally generated. Due primarily to the difficulties inherent in detailed structural analysis of gel-phase systems, this suggestion has not yet been subjected to rigorous investigation. The fact that zeolitic materials are often detected in geopolymeric systems suggests that this proposal is definitely worthy of further study.

1.2 CRYSTALLINITY IN GEOPOLYMERS

Hydrothermal synthesis from calcined clays, particularly metakaolin (calcined kaolinite), has long been used in the production of low-silica zeolites. The physicochemical conditions under which zeolites are obtained from metakaolin are very similar to those used in geopolymerisation. Temperature and water content are generally higher in zeolite synthesis systems than in geopolymerisation, but there is no clear distinction between the conditions under which each product is obtained. An indication of the products obtained under different conditions is given in Table 1. Approximate dividing lines between 'low' and 'high' temperature may be drawn at approximately 40-80°C, and between 'low' and 'high' water content at H_2O/M_2O ratios of around 10-20. However, the distinctions between 'low' and high' values of each parameter are left intentionally vague as the exact nature of the products formed is subject to other synthesis variables, particularly Si/Al ratio and reaction time. In general, longer reaction times tend to give more crystalline products. Activation of metakaolin with alkali metal silicate rather than hydroxide solution tends to give geopolymeric rather than highly crystalline zeolitic products at high temperature and low water content, and in most cases gives a product of a higher compressive strength.

Table 1. The products formed by hydrothermal treatment of solid aluminosilicates at different temperatures and water contents

		Temperature	
		Low	High
Water content	Low	Geopolymer [a]	Geopolymer [b] or zeolite [c]
	High	Aluminosilicate gel [d]	Zeolite [e]

[a] : van Jaarsveld *et al.* (1997), Cioffi *et al.* (2003)

[b] : Davidovits (1991), Bao *et al.* (2003), Krivenko and Kovalchuk (2002)

[c] : Akolekar *et al.* (1997), Walton *et al.* (2001)

[d]: Dutta *et al.* (1987), Subotić *et al.* (1994)

[e]: Barrer (1966), Ciric (1968), Davis and Lobo (1992)

Suggestions of a correspondence between geopolymerisation and zeolite synthesis have been strengthened by the use of high-resolution microscopic techniques to observe phase formation within geopolymeric binders. Transmission electron microscopy (TEM) has shown the geopolymer phase to be nanoparticulate, with many particles approximately 5nm in diameter surrounded by what is either a secondary continuous phase, regions of nanoporosity, or a mixture of the two (van Jaarsveld 2000; Gordon *et al.* 2004). Electron diffraction studies of geopolymers show regions displaying varying degrees of crystallinity, ranging from highly crystalline, nanocrystalline or polycrystalline through to fully amorphous, but indexing of the diffraction patterns has never yet been carried out. High-resolution electron microscopy (HREM) shows that the particulate phase contains distinct regions of short- to mid-range order, which are rapidly amorphised by beam damage (van Jaarsveld 2000). The observed structures and behaviour resemble the structures and amorphisation process first noted by Bursill *et al.* (1980) in their HREM investigation of zeolite A.

The major feature of XRD powder diffraction patterns of geopolymers is a largely featureless 'hump' centred at approximately 27-29° 2θ. An example of a typical geopolymer X-ray diffractogram is provided in Figure 1. Numerous other examples may be found in the literature. However, the most outstanding feature of all published diffractograms of geopolymers is that, regardless of the choice of solid aluminosilicate source (metakaolin with or without added calcium, fly ash or blast furnace slag), activating solution (sodium or potassium hydroxide at different concentrations, with or without soluble silicate), and curing conditions (time, temperature and humidity), the broad hump centred at around 27-29° 2θ is present in every case.

This ubiquitous peak must therefore be considered the distinguishing feature of the diffractogram of any geopolymer, and so its identification becomes central to the determination of the microstructure of a geopolymer.

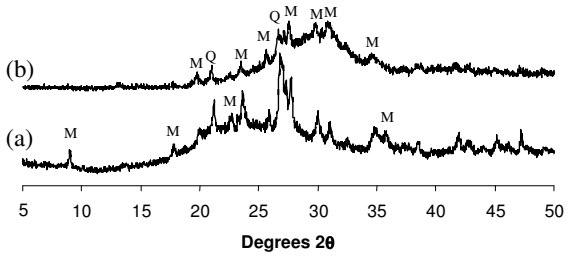

Figure 1. Cu-Kα X-ray diffractograms of (a) metakaolin (MetaStar 501, Imerys, UK), and (b) a metakaolin/potassium silicate geopolymer with nominal composition $K_2O{\cdot}Al_2O_3{\cdot}2.65SiO_2$, cured at 70°C for 24h. All crystalline peaks are assigned to impurities in the metakaolin: muscovite (M) and quartz (Q).

Sometimes described as a 'diffuse halo peak' (Davidovits 1991), this broad hump is generally attributed to the amorphous aluminosilicate gel assumed by most authors to be the primary binder phase present in geopolymeric systems. However, high-resolution microscopy of geopolymeric systems has shown this gel phase to be present largely in the form of nanosized aluminosilicate particles (van Jaarsveld 2000; Yip *et al.* 2003; Kriven *et al.* 2004), which in some cases show significant crystallinity under electron diffraction.

However, it is common that no newly formed crystalline phases are identifiable in X-ray diffraction (XRD) analysis of geopolymeric products. It can be deduced from these seemingly conflicting results that the crystallinity observed in the HREM and electron diffraction experiments is present on a length scale below the detection limit of XRD. Similar apparent discrepancies between XRD and electron diffraction results have been noted in studies of aluminosilicate zeolite precursor gels (Subotić *et al.* 1994), as well as in a variety of other inorganic systems. In several investigations, crystallinity on a length scale of around 5nm was detectable by electron diffraction experiments but not by XRD. This correlates very well with the observed presence of 5nm particulates with varying degrees of crystallinity within the geopolymeric binder phase, and provides a plausible explanation for a series of apparently

contradictory results present in the literature. Several studies of aluminosilicate crystallisation kinetics have also quantitatively displayed the instrumental limitations on XRD crystallinity analysis by comparison of the development of the degree of crystallinity calculated from FTIR (Jacobs *et al.* 1981; Akolekar *et al.* 1997) or DTA (Gabelica *et al.* 1983) with corresponding XRD results.

The research programme led by Subotić (Subotić *et al.* 1994; Antonić and Subotić 1998) has shown that the amorphous precursor gels from which zeolites are crystallised in fact contain many 'quasicrystalline' regions, which act as sites for zeolite nucleation as the gel dissolves. Mintova *et al.* (1999a; b) have also shown that zeolite growth from gel precursors begins with the formation of nanosized crystallites within the amorphous gel particles. These crystallites resemble the ordered domains observed in HREM images of geopolymeric binders, adding further support to the proposition that geopolymers contain a significant level of nanoscale crystallinity in the form of zeolitic nanocrystals.

This information may then be used to provide an explanation for the observed properties of geopolymers: nanocrystalline regions within the nanosized particulate phase observed under TEM will give electron diffraction patterns typical of crystalline structures, while being ordered on a length scale too short to provide the characteristic X-ray diffractograms of their actual crystal structure. As the crystalline state minimises the free energy of a system, the formation of crystalline regions via the dissolution-reprecipitation process of geopolymerisation is not unexpected, but identification of the chemical nature of these regions remains a point of some contention. Despite the complications inherent in analysis of diffractograms of 'amorphous' materials, significant conclusions may still be reached by careful investigation and comparison of the existing published results in this field.

Figure 2 (Akolekar *et al.* 1997) shows a time-resolved sequence of powder X-ray diffractograms detailing the transformation of metakaolin to zeolite X in mixed KOH/NaOH solution at 51°C. As in the case of zeolite synthesis from colloidal silica and sodium aluminate and also in other investigations of zeolite formation by leaching of metakaolin (Rocha *et al.* 1991), a broad peak centred at approximately 28° 2θ is seen in diffractogram a in Figure 2.6 to replace the initial 22° peak early in the transformation of metakaolin to the zeolite product. Peaks characteristic of zeolite A, most notably at ~7° 2θ, are observed in addition to the 'amorphous

hump' in the intermediate stages of the reaction (diffractograms b and c). However, these peaks decrease in intensity as zeolite X, the preferred product under the relatively low temperatures used (Cournoyer *et al.* 1975; Šefčík and McCormick 1999), is formed. This is in accordance with the accepted applicability of Ostwald's law of successive reactions to zeolite synthesis systems (Davis and Lobo 1992). Davidovits (1988) and Benharrats *et al.* (2003) each obtained corresponding results in the reaction of kaolin or metakaolin with NaOH at 150°C and 80°C respectively, with zeolite A formed initially in each case and hydroxysodalite increasingly prominent as the reaction continued.

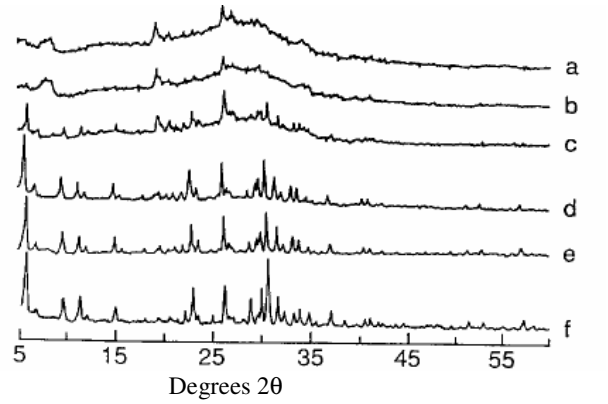

Figure 2. Cu-Kα X-ray diffractograms of the products of leaching metakaolin extrudates with mixed NaOH/KOH solution at 51ºC for (a) 6h, (b) 24h, (c) 48h, (d) 72h, (e) 96h, and (f) 240h. From Akolekar *et al.* (1997).

The presence of multiple zeolitic species in the reaction system of Akolekar *et al.* (1997), with conditions similar to those under which geopolymerisation is carried out, suggests that a variety of zeolitic species will also be present in geopolymeric products. Authors identifying particular zeolites within a geopolymeric matrix have noted the presence of hydroxysodalite, faujasites (zeolites X and/or Y), and zeolite A, with zeolite formation favoured at lower activating solution Na_2O/SiO_2 ratio (Rahier *et al.* 1997) and higher temperature (Palomo and Glasser 1992).

Phair *et al.* (2001) stated that "crystallinity cannot yet be excluded as a means of strength development in geopolymeric systems." Far from excluding crystallinity as a means of strength development, information obtained by considering geopolymers as agglomerates of nanometre-scale crystal nuclei bound together by an amorphous gel phase may now be used to reinterpret and explain previously inexplicable experimental results. However, before this can be done these

results must be re-examined with a view to reconciling various sets of seemingly contradictory data that have been published in the field of geopolymers and geopolymerisation.

1.3 ANALYSIS OF MECHANICAL STRENGTH RESULTS

The most commonly employed measure of the success or otherwise of a geopolymerisation process is the compressive strength of the final product. This is primarily due to the low cost and simplicity of compressive strength testing, and the importance of strength development as a primary measure of the utility of materials in different applications in the construction industry.

Several highly significant results regarding chemical structure may be obtained from existing mechanical strength data. In particular, the importance of the charge-balancing role of cations within a geopolymeric structure is exemplified by Figure 3. This figure displays a sharp maximum in both compressive and tensile strength at a Na/Al ratio of exactly 1, corresponding to a single Na^+ cation balancing the charge on each tetrahedral Al centre.

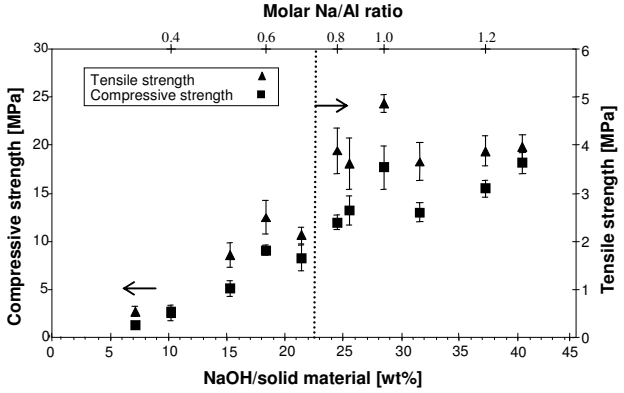

Figure 3. Influence of the Na/Al ratio on the mechanical properties of geopolymers formed by activation of metakaolin with NaOH solutions of differing concentrations, cured at 35°C for 24h. Data from Kaps and Buchwald (2002).

Corresponding but less detailed results for sodium silicate activation of metakaolin have also been published by Rahier *et al.* (1996b). This observation also corresponds to the assertion of Barrer and White (1952) that Na/Al ratios of exactly 1 favoured the formation of framework (Q^4)

aluminosilicate materials during hydrothermal synthesis, where ratios higher or lower than this either gave lower yields or different products.

The requirement for a particular stoichiometric M^+/Al ratio to achieve maximum strength in geopolymeric binders adds further support to the proposal presented in the thesis that these binders display a significant degree of chemical ordering, and nanocrystallinity in particular. All the crystalline zeolitic structures previously mentioned as having been identified within geopolymeric binders require full charge-balancing by one alkali metal cation for each tetrahedral Al centre. In contrast, amorphous structures do not show such strong charge-balancing requirements, as their less-ordered nature allows variation from strict tetrahedral geometry and therefore allows methods of charge compensation other than strict association of a single alkali metal cation with each Al centre.

1.4 ANALYSIS OF CALORIMETRIC DATA

Another quantitative analytical method commonly used in the analysis of the geopolymerisation process is calorimetry. Data have been gathered by techniques including differential scanning calorimetry (DSC) and isothermal conduction calorimetry (ICC). The most important results obtained to date from calorimetric experiments generally fall into one of two categories: (1) determination of the correspondence between degree of reaction and physical properties, and (2) elucidation of the mechanism of reaction. As the mechanism of geopolymerisation is an area requiring considerably more study before definitive conclusions may be reached, the primary focus of this section will be the use of existing calorimetric data in conjunction with the nanocrystallinity hypothesis to describe the observed physical properties of geopolymers.

The data of Rahier *et al.* (1996b) presented in Figure 4 illustrate most clearly the relationship between degree of reaction and mechanical properties of a geopolymer. As all stages of the reaction between metakaolin and alkali silicate solution have been observed in ICC experiments to be exothermic (Alonso and Palomo 2001a), reaction enthalpy may be used as a direct representation of the extent of the reaction (Granizo *et al.* 2000). Figure 4 shows a linear relationship, exact to within experimental error margins, between reaction enthalpy and product

compressive strength. This corresponds with the absence of any observable aggregate effect in alkali-activated metakaolin systems due to the low hardness of metakaolin.

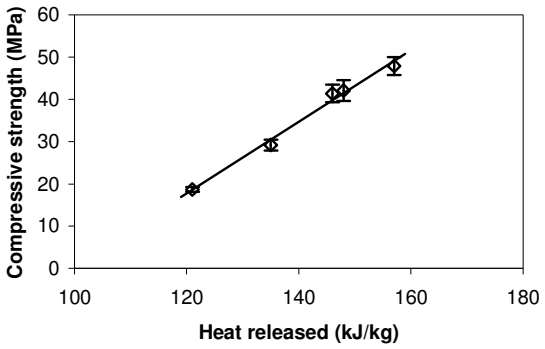

Figure 4. Relationship between total reaction enthalpy and product strength in geopolymers formed by activation of metakaolin with sodium silicate. Error bars represent one standard deviation. Data from Rahier *et al.* (1996b).

In contrast, fly ash-based systems display no such clear general trend due to the compositional and physical differences between fly ashes from different sources, or even between different batches of ash from the same source (van Jaarsveld *et al.* 2003).

A combination of calorimetric and FTIR data has been used to show that the degree of formation of crystalline materials generally increases with increasing alkali concentration in the NaOH activation of metakaolin/$Ca(OH)_2$ mixtures (Granizo *et al.* 2002). This high alkalinity also tends to give delayed setting, particularly in the absence of dissolved silicates in the initial activating solution. A source of some confusion in the comparison of these data with those plotted in Figure 2.11 (Rahier *et al.* 1996b) is the reversal of the strength/heat release relationship observed in Figure 2.11; with the investigation of Alonso and Palomo (2001a) instead showing the samples with the highest heat release had the lowest strength. However, the presence of high levels of calcium in the reaction mixtures used by Alonso and Palomo renders any direct comparison with the data of Rahier *et al.* (1996b) impossible. Addition of significant levels of calcium to a geopolymer-forming system has been shown to give a phase-mixed C-S-H/amorphous aluminosilicate material rather than the zeolite-gel systems formed in the absence of calcium (Yip and van Deventer 2003). This will be expected to display very different synthesis

pathways leading to its quite distinct microstructure, meaning that the heat release/strength relationships are not expected to be comparable to calcium-free systems.

1.5 THE IMPORTANCE OF CRYSTALLINITY

The identification of nanocrystalline zeolitic materials embedded in an amorphous aluminosilicate gel phase as a significant component of geopolymeric materials is not entirely unexpected. An explanation for the differences in crystallinity observed in geopolymers activated with different levels of soluble silicate is now possible, with the differing rates of nucleation and crystal growth in each scenario playing a large part in determining the physicochemical and engineering properties of the products in each case. The observation of Rahier *et al.* (1997) that crystallinity decreases as more silicate is added to the activating solution in geopolymerisation is justifiable from a theoretical standpoint. However, with nucleation not happening in such close proximity to the particle surfaces in hydroxide-activated as in silicate-activated geopolymers, the binding of the particles into the geopolymeric matrix is likely to be less strong, and so the mechanical strength of the product developed by activation with hydroxides is lower than with silicates (Rowles and O'Connor 2003). It is not yet clear whether the compositional dependence of the degree of crystallisation is due simply to the higher pH of the low-silica activating solutions, or whether the particular zeolite framework types being formed have a significant influence.Control of the crystallisation behaviour of geopolymers will be of significant benefit in the use of these materials in immobilisation of wastes containing high levels of alkali or alkaline earth metals, which are known to participate selectively in ion exchange reactions on particular zeolites. Tailoring of the particular zeolite crystal structures formed within a geopolymeric binder to ensure optimal immobilisation of the desired contaminant may therefore be possible.

The effects of temperature and alkalinity on geopolymerisation can also be partially explained by the description of a geopolymer as an agglomerate of zeolite nuclei within a gel matrix. Increasing the temperature of a chemical reaction system will increase the rate of the reactions occurring according to the standard Arrhenius expression, which will be shown later in this report to be applicable in a general sense to the analysis of geopolymerisation. However, increases in either temperature or alkalinity of a geopolymer-forming mixture will also increase the solubility of aluminosilicate species in the aqueous phase, so a lower degree of supersaturation will be present at any given aluminosilicate concentration. This will slow both nucleation and crystal

growth, with differing effects on the crystallinity of the product. Presence of more nuclei will give a less crystalline product as the higher degree of competition for the nutrients required for crystal growth leads to a smaller average crystal size and therefore lower apparent crystallinity, while the presence of fewer nuclei will give larger crystals and slower solidification. Larger crystals will be less able to pack densely within the binder phase, so will give a more porous geopolymer. Such a decrease in density with increasing curing temperature has been observed experimentally by Cioffi *et al.* (2003). Depending on the exact nature and crystallite size of the product and the strength of the bonds between the crystalline nuclei and the surrounding material, the strength of the geopolymeric matrix could therefore either decrease or increase with increasing curing temperature, as has been previously observed.

2. FRAMEWORK CATION ORDERING

The work summarised in this section was published in the papers Duxson *et al.* (2005a) and Provis *et al.* (2005a), as well as Chapter 6 of the Ph.D. thesis of Peter Duxson, submitted for examination at the University of Melbourne, 24 February 2006. Full derivations of the equations used, as well as complete NMR data sets, are published in these papers and will not be repeated in detail in this report.

2.1 INTRODUCTION

The distribution and short-range (chemical) ordering of silicon and aluminium within tetrahedral framework structures has been the subject of significant work, and often controversy, for over 50 years (Loewenstein 1954). However, such calculations have never before been applied to geopolymeric materials, with the amorphicity of these materials and the lack of reliable data regarding atomic configurations within the binder phase combining to make such analysis very difficult. The partially-reacted raw materials present in geopolymers also cause some difficulties as will be discussed later in this chapter. With a view towards potential applications in radioactive waste treatment, understanding of the degree of chemical ordering in geopolymers, which will play a significant role in determining the long-term chemical stability of these systems, is critical.

Short-range order in aluminosilicate materials such as zeolites, minerals and glasses has been investigated with great success using NMR spectroscopy (Klinowski 1984; Phillips *et al.* 1992; Lee and Stebbins 1999). The lack of spectral resolution for silicon in glassy and amorphous materials similar in chemistry to geopolymers has been overcome by adopting Gaussian peak deconvolution to separate and quantify the different possible coordinations of Si with respect to Al (Engelhardt and Michel 1987; Lee and Stebbins 1999). Quantification of network ordering has allowed development of models for describing speciation of silicon (Ramdas *et al.* 1981; Klinowski *et al.* 1982). Recent investigations of alkali aluminosilicate glasses and minerals have identified the existence of significant quantities of Al-O-Al bonding, forcing a paradigm shift from the assumption of explicit adherence to Loewenstein's Rule (Lee and Stebbins 2000). No such detailed investigations of geopolymeric gel systems have previously been reported. Here,

deconvolution of ^{29}Si MAS-NMR spectra by curve-fitting of Gaussian lineshapes is found to provide meaningful information regarding the distribution of silicon and aluminium tetrahedra within the geopolymeric binder.

The notation introduced by Engelhardt *et al.* (1982) will be followed in this work, with $Q^n(m\text{Al})$ $(0 \leq m \leq n \leq 4)$ representing a silicate centre coordinated to n other tetrahedral centres, of which m are aluminium and $(n\text{-}m)$ are silicon. Similarly, $q^{n'}(m'\text{Al})$ $(0 \leq m' \leq n' \leq 4)$ will be used to represent an aluminium centre coordinated to n other tetrahedral centres, of which m are aluminium and $(n\text{-}m)$ are silicon. The presence of non-bridging oxygens in geopolymeric systems is considered negligible, with all tetrahedral sites being observed by NMR to have cross-link density $n = 4$ (Rahier *et al.* 1996b; Barbosa *et al.* 2000). This observation will be utilised throughout model development and analysis to simplify the discussion of bond distribution, with $n = 4$ taken to be constant.

The standard starting point in short-range structural analysis of aluminosilicates is Loewenstein's rule (Loewenstein 1954), which states that no two aluminium ions can occupy the centres of tetrahedra linked by one oxygen. This 'rule' is often assumed, either explicitly or implicitly, to be obeyed strictly in aluminosilicate structures. However, there is no theoretical basis for strict application of aluminium avoidance, but rather a thermodynamic preference giving a strong tendency towards avoidance of Al-O-Al bonds. Free energy minimisation considerations may therefore be used to interpret the observed tendency towards Al-O-Al avoidance in aluminosilicate structures. The unfavourable formation of Al-O-Al bonds in solution is believed to be largely responsible for the short-range ordering of silicon and aluminium centres in hydrothermally synthesised aluminosilicates (Catlow *et al.* 1996). Significant degrees of Si/Al disorder have been observed in melt-quenched glasses, synthetic feldspars and natural minerals. A Monte Carlo simulation of Si/Al ordering in ultramarines over a wide range of synthesis temperatures (Gordillo and Herrero 1992) showed a sudden decrease in ordering at approximately 500°C, with the high-temperature regime producing essentially random ordering. Similar temperature effects were incorporated into the simple statistical model of Lee and Stebbins (1999) via a Boltzmann-type exponential term.

The free-energy model for chemical ordering of tetrahedral sites in alloys (Efstathiadis *et al.* 1992), based on Gibbs energy minimisation with explicit consideration of both enthalpic and entropic effects, is adapted and applied to the description of aluminosilicates in general, using

geopolymers as a model system. The validity of the application of this model, originally presented in the description of Si-C-H ordering in amorphous hydrogenated silicon carbide alloys, to the inorganic polymer network structure will be discussed. The implication of this applicability is that the model is suitable for use in the study of bond ordering in other amorphous aluminosilicate materials, as the model does not require prior knowledge of the framework structure of the material.

2.2 EXPERIMENTAL METHODS

Full experimental details are presented by Duxson *et al.* (2005a), and are summarized briefly here. A commercial metakaolin, MetaStar 402 (Imerys, Bristol UK), with molar composition determined by X-ray fluorescence (XRF) to be $2.3SiO_2 \cdot Al_2O_3$, was used in the synthesis of all samples unless sotherwise noted. For ^{17}O 3QMAS-NMR spectroscopy, use of a pure precursor was desirable, so a synthetic chemically pure aluminosilicate powder with composition $(2:1)SiO_2.Al_2O_3$ was provided by the Kriven research group (University of Illinois at Urbana-Champaign). Details of powder preparation by the PVA method are provided elsewhere (Nguyen *et al.* 1999). Alkali metal silicate solutions with H_2O/M_2O = 11 (M: alkali metal) and different ratios Na/(Na+K) = 0.0, 0.5 and 1.0, and SiO_2/M_2O = 0.0, 0.5, 1.0, 1.5 and 2.0, were prepared by fully dissolving fumed silica in appropriate hydroxide solutions.

Geopolymer specimens were prepared by mechanically mixing the metakaolin and silicate solutions to form a homogeneous slurry with Al_2O_3/M_2O = 1, shaking to remove bubbles, and curing in sealed Teflon moulds at 40°C for 20h. Specimens containing only sodium cations will be referred to as Na-geopolymers, while those with sodium and potassium (1:1) or only potassium cations will be referred to as NaK- and K-geopolymers respectively. Samples prepared from PVA-method precursors are described as Na-PVA and K-PVA samples.

^{29}Si NMR spectra were obtained at a Larmor frequency of 59.616 MHz with a Varian (Palo Alto, CA) Inova 300 NMR spectrometer (7.05 T). Powdered specimens were packed into 5 mm zirconia rotors for a Doty (Columbia, SC) broadband MAS probe. Spectra were acquired at spinning speeds of 5 kHz with peak positions referenced to an external standard of tetramethylsilane (TMS). 1024 transients were acquired using a single $\pi/2$ (4.8 μs) pulse and

recycle delays typically 15-30s, being at least 5 times T_1 as measured by the saturation recovery method. 50 Hz line broadening was applied to all spectra. Full details of the deconvolution procedure, and detailed analysis of the results obtained, are given by Duxson *et al.* (2005a).

Solid-state ^{17}O NMR spectroscopy was performed at 19.6 T (112.43 MHz for ^{17}O nuclei) at the National High Magnetic Field Laboratory (Tallahassee, Florida), using a Bruker DRX spectrometer and a 4-mm MAS probe. All ^{17}O chemical shifts were referenced to tap water. Spinning speeds for MAS and MQMAS experiments were 10 kHz. ^{17}O 3QMAS NMR spectra were collected using a shifted-echo pulse sequence composed of two hard pulses with duration of 3.5 μs and 1.5 μs. The recycle time for all experiments was 0.2 s. The Hahn-echo was used to obtain 1D spectra. Spectra of all specimens were recorded in the as-cured state and after drying to remove isotropic contributions from pore solution. MQMAS spectra were analysed by performing 2D Fourier transformations by a factor of 19/12 to yield 2D spectra with either an isotropic component along the F1 spectral axis and an anisotropic component along the F2 axis (Massiot *et al.* 1996), or by 3 to provide a pure quadrupolar component along the F1 axis.

2.3 NMR AND DECONVOLUTION RESULTS

The ^{29}Si MAS NMR spectra of geopolymers show a broad resonance centered at –85 to –93 ppm, consistent with previous observations (Davidovits 1991). Figure 5 shows a set of spectra obtained from Na-geopolymers, as well as the results of deconvolution of these spectra; NaK- and K-geopolymers give similar results (Duxson *et al.* 2005a).

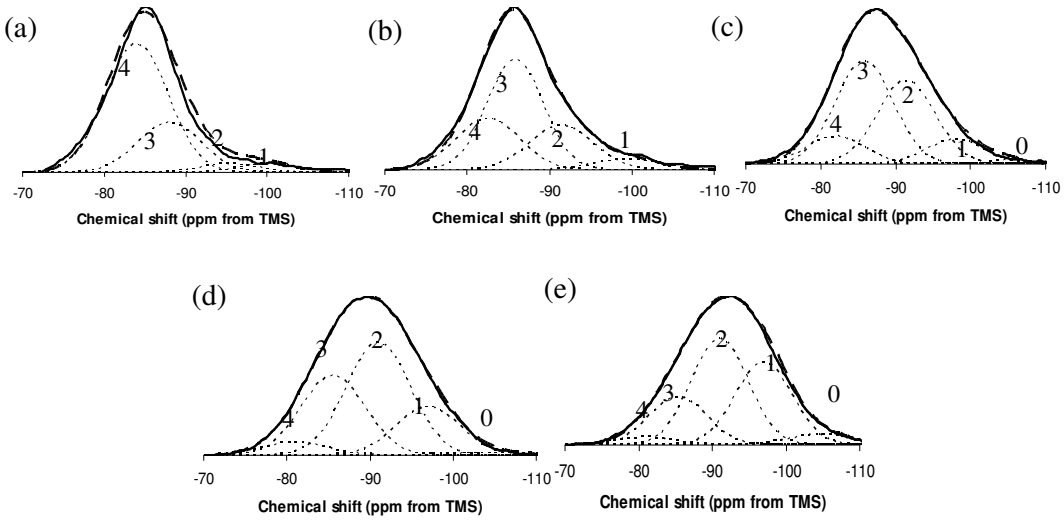

Figure 5. Deconvoluted ^{29}Si MAS NMR spectra of Na-geopolymers with compositions (a) x = 0.535, (b) x = 0.589, (c) x = 0.632, (d) x = 0.669, and (e) x = 0.699. Solid lines are experimental spectra, thin dotted lines are the contributions of each site type (denoted by values of m), and thick dashed lines are the total calculated spectra.

2.4 STATISTICAL THERMODYNAMIC MODEL

The model presented here is developed from the work of Efstathiadis *et al*. (1992), and full derivations of all equations are presented elsewhere (Provis *et al.* 2005a). This model was originally implemented for 3-component Si-C-H alloy, with the 2-component Si-C system discussed in detail. Here, the model will be derived purely on a 2-component basis, describing the ordering behavior of tetrahedral $SiO_{4/2}$ and $AlO^-_{4/2}$ centers. This particular model was chosen largely because it does not rely on a knowledge of the network topology, which is currently unavailable for geopolymers due to their X-ray amorphous nature. This also provides the potential for its applicability to other amorphous aluminosilicate systems including glasses.

Chemical ordering in geopolymers is due primarily to the exothermicity of Equation (1), where Ω is the energy released by the reaction depicted. The value of Ω is dependent on the non-framework cations present and the topology of the tetrahedral network structure, and so is treated as a model parameter here. Next-nearest neighbor Si/Al substitution has been calculated to contribute approximately ±20% to the value of Ω (Palin *et al.* 2001). However, this effect is

commonly neglected in modeling. It is also not possible to give a full description of next-nearest-neighbor effects without knowledge of the network topology, which is not available for geopolymers due to their amorphicity. Therefore, this effect will not be considered explicitly here.

$$\left[\equiv \text{Si-O-Si} \equiv\right] \quad + \quad \left[\equiv \text{Al-O-Al} \equiv\ \right] \quad \Leftrightarrow \quad 2\left[\equiv \text{Si-O-Al} \equiv\right] \quad + \quad \Omega \qquad (1)$$

The Gibbs free energy of mixing (network formation), G_M, is expressed in terms of the entropy and enthalpy of mixing:

$$G_M = H_M - TS_M \qquad (2)$$

The entropy of mixing is given by the Boltzmann equation, Equation (3):

$$S_M = k_B \ln \Gamma \qquad (3)$$

where k_B is Boltzmann's constant and Γ is the number of distinct states the system may occupy. Enumerating these states and discarding terms which are negligible compared to the very large factorial terms generated then gives Equation (4), which holds asymptotically in the limit of large N. This equation describes a system of N framework sites, $N(\text{Si}) = xN$ of which are silicon and $N(\text{Al}) = (1\text{-}x)N$ are aluminum. $N_{I,J}$ is defined as the concentration of centers of type I bonded via I-O-J bonds to sites of type J, and $N_{Al,Si} = N_{Si,Al}$.

$$S_M \sim 4k_B \ln\left(\frac{N(\text{Si})!\,N(\text{Al})!}{N_{Si,Si}!\,N_{Al,Al}!\left(N_{Si,Al}!\right)^2}\right) \qquad (4)$$

Applying Stirling's approximation to the factorials and expressing in terms of 'normalized bond concentrations' $n_{I,J} = N_{I,J}/N(\text{Si})$ and $x = N(\text{Si})/N_{total}$ yields Equation (5):

$$S_M = -4k_B N(\text{Si})\left[n_{\text{Si,Si}} \ln\left(n_{\text{Si,Si}}\right) + n_{\text{Al,Al}} \ln\left(n_{\text{Al,Al}}\right) + 2n_{\text{Si,Al}} \ln\left(n_{\text{Si,Al}}\right) + \frac{1-x}{x} \ln\left(\frac{x}{1-x}\right)\right] \qquad (5)$$

The enthalpy of mixing may be expressed in terms of heats of formation of free tetrahedra $H_0(\text{I})$ and bond energies $E(\text{I-O-J})$ by Equation (6) (Efstathiadis *et al.* 1992), developed by

considering each tetrahedral site in turn and summing the contributions of the bonds from it to its neighbors.

$$\begin{aligned} \mathrm{H_M} \;=\; & N(\mathrm{Si})\;[\mathrm{H_0}(\mathrm{SiO_{4/2}}) + \frac{1-x}{x}\mathrm{H_0}(\mathrm{MAlO_{4/2}}) - 2n_{Si,Si}\mathrm{E}(\mathrm{Si-O-Si}) \\ & - 4n_{Si,Al}\mathrm{E}(\mathrm{Si-O-Al}) - 2n_{Al,Al}\mathrm{E}(\mathrm{Al-O-Al})] \end{aligned} \tag{6}$$

Combining Equations (2), (5) and (6) gives Equation (7), a detailed expression for the Gibbs energy of the system:

$$\begin{aligned} \mathrm{G_M} = {} & N(\mathrm{Si})\left[\mathrm{H_0}(\mathrm{SiO_{4/2}}) + \frac{1-x}{x}\mathrm{H_0}(\mathrm{MAlO_{4/2}}) - 2n_{Si,Si}\mathrm{E}(\mathrm{Si-O-Si}) - 4n_{Si,Al}\mathrm{E}(\mathrm{Si-O-Al}) - 2n_{Al,Al}\mathrm{E}(\mathrm{Al-O-Al})\right] \\ & - 4Tk_{\mathrm{B}}N(\mathrm{Si})\left[n_{\mathrm{Si,Si}}\ln(n_{\mathrm{Si,Si}}) + n_{\mathrm{Al,Al}}\ln(n_{\mathrm{Al,Al}}) + 2n_{\mathrm{Si,Al}}\ln(n_{\mathrm{Si,Al}}) + \frac{1-x}{x}\ln\left(\frac{x}{1-x}\right)\right] \end{aligned} \tag{7}$$

Differentiating with respect to $n_{Si,Si}$ then yields Equation (8):

$$\frac{\partial \mathrm{G_M}}{\partial n_{Si,Si}} = -2\Omega N(\mathrm{Si}) - 4k_{\mathrm{B}}T \cdot N(\mathrm{Si})\left[\ln(n_{\mathrm{Si,Si}}) + \ln(n_{\mathrm{Al,Al}}) - 2\ln(n_{\mathrm{Si,Al}})\right] \tag{8}$$

Setting $\frac{\partial \mathrm{G_M}}{\partial n_{Si,Si}} = 0$ and rearranging:

$$\frac{n_{Si,Al}^2}{n_{Si,Si}n_{Al,Al}} = \exp\left(\frac{\Omega}{2k_{\mathrm{B}}T}\right) \tag{9}$$

Combining Equation (9) with the fundamental bond concentration relationships for a binary system (Equations (10) and (11)) and solving algebraically, Equation (12) is obtained. This is an analytical expression for the degree of Si-O-Al bonding in terms of the system composition, bond energy penalty and synthesis temperature (set at 40°C throughout this work (Duxson *et al.* 2005a)).

$$n_{\mathrm{Si,Si}} + n_{\mathrm{Si,Al}} = 1 \tag{10}$$

$$n_{\mathrm{Si,Al}} + n_{\mathrm{Al,Al}} = \frac{1 - x}{x} \tag{11}$$

$$n_{\mathrm{Si,Al}} = \frac{\frac{1}{x}\exp\left(\frac{\Omega}{2k_{\mathrm{B}}T}\right) - \sqrt{\left(\left(\frac{1}{x} - 2\right)\exp\left(\frac{\Omega}{2k_{\mathrm{B}}T}\right) + 2\right)^2 + 4\left(\exp\left(\frac{\Omega}{2k_{\mathrm{B}}T}\right) - 1\right)}}{2\left(\exp\left(\frac{\Omega}{2k_{\mathrm{B}}T}\right) - 1\right)} \tag{12}$$

Equations (10)-(12) may then be used to calculate the total number of each type of bond present in the system for given x and Ω. The distribution of these bonds is assumed to be random, neglecting next-nearest neighbor effects as noted earlier. This then allows the calculation of $F_{Si}(m)$, the fraction of all tetrahedra that are $Q^4(m\mathrm{Al})$, by Equation (13).

$$\mathrm{F_{Si}}\left(m\right) = \binom{4}{m} x\, n_{Si,Al}^{m}\, n_{Si,Si}^{4-m} \tag{13}$$

2.5 APPLICATION OF THE MODEL TO EXPERIMENTAL DATA

Fitting the model to experimental data requires the estimation of the energy penalty Ω for each set of data. A discussion of the range of values of Ω presented in the literature is presented by Provis *et al.* (2005a), and additional values are presented in the review of Bosenick *et al.* (2001). The literature data suggest that Ω values in the range approximately 20-50 kJ/mol are to be expected in aluminosilicate structures, which will provide a check on the validity of the model presented here. Myers (1999) found that the energy penalty for a 1:1 mixed cation system is approximately equal to the mean of the endmember values. This observation will be used here in the analysis of the mixed NaK-geopolymer system, where Ω will be taken to be the mean of the values selected for the pure Na and K systems. These parameters must themselves be estimated by simply choosing the value of Ω that gives the best fit to the experimental data for each pure system.

For this model to be applied accurately to a geopolymeric system, it must be noted that there remains some quantity of unreacted metakaolin within the geopolymeric gel binder phase. This remnant metakaolin will have a different composition to the surrounding binder phase, meaning

that the actual composition of the newly-formed geopolymeric binder will not correspond exactly to the superficial (nominal) composition. Therefore, a composition correction will be required for the model to accurately represent the actual geopolymeric binder phase. The work of Duxson *et al.* (2005b) in calculating the extent of reaction in metakaolin-based geopolymers of different silica contents from ^{27}Al MAS NMR results will be utilized here. However, these results provide only a relative measure of the extent of reaction across a range of samples. It is therefore necessary to estimate a starting point from which to convert the relative data into absolute extents of reaction. From the ^{29}Si MAS NMR spectrum obtained at x = 0.535, approximately 10% remnant metakaolin is observed, visible as a Q^4(1Al) peak in the deconvolution. This value is then used to scale the relative extent of reaction data of Duxson *et al.* (2005b) throughout this work.

It has been observed that the initial stage of dissolution of many aluminosilicate minerals and clays in alkaline solution displays preferential release of aluminum, leading to silica-enrichment of the undissolved material (Walther 1996). It is therefore reasonable to expect similar behavior during geopolymerization, with preferential leaching of Al from the metakaolin leading to Si-enriched remnant particles within a slightly Al-rich binder phase. For modeling purposes, it has been estimated that the remnant metakaolin will have a composition of x = 0.600, compared to its original composition of x = 0.535. Model results are therefore compared to experimental data by use of a corrected composition x_{corr}, enabling the model to describe ordering according to the actual binder composition rather than the superficial sample composition.

2.6 Model Results and Discussion

Figure 6 shows the application of the statistical thermodynamic model to the experimental ^{29}Si MAS NMR data (Duxson *et al.* 2005a) for Na, K and mixed Na/K metakaolin-based geopolymers respectively. Ω was found to be 40 (±5) kJ/mol for Na geopolymers and 30 (±2) kJ/mol for K geopolymers, giving Ω = 35 kJ/mol for the mixed Na/K system. It is observed that the model is generally applicable to description of the Si/Al ordering behavior of geopolymers, and that the parameter values fall within the range expected based on the available literature data. This further validates the modeling approach used, and provides a means of atomic-scale comparison between geopolymers and other aluminosilicates.

(b)

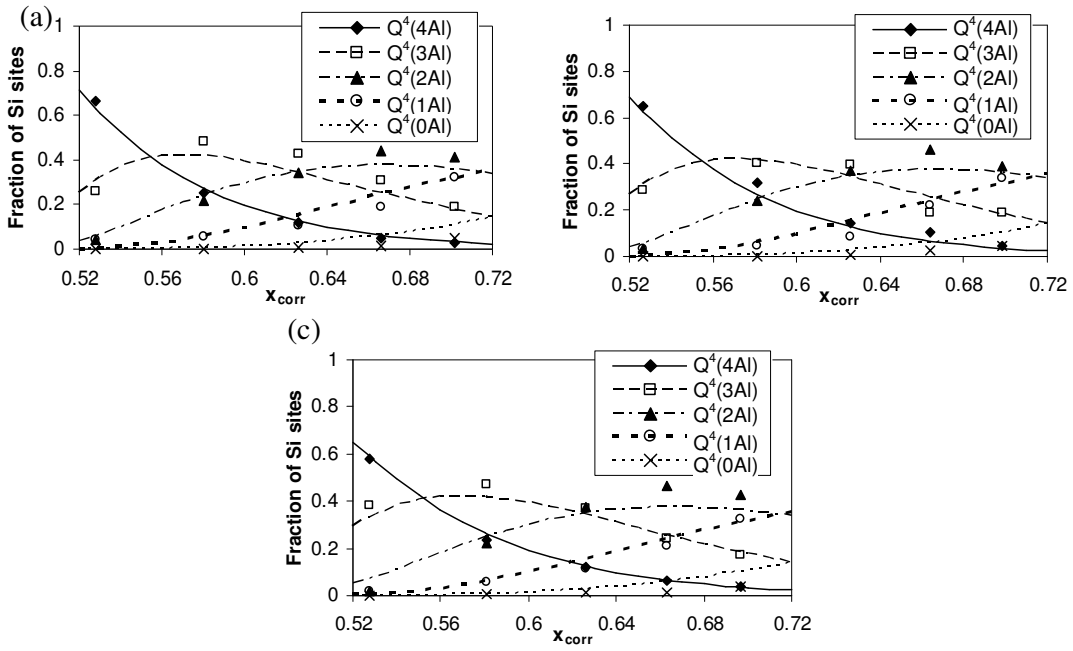

Figure 6. Comparison of model predictions to experimental data with composition corrections, for (a) Na-geopolymers, Ω = 40 kJ/mol, (b) K-geopolymers, Ω = 30 kJ/mol, and (c) mixed (1:1) NaK-geopolymers, Ω = 35 kJ/mol. Lines represent model predictions, and points experimental data.

Other than uncertainties due to unreacted metakaolin, the main possible source of error in the application of this model is likely to be next-nearest-neighbor effects. Dempsey's rule (Dempsey *et al.* 1969) predicts that Al-O-Si-O-Al bonds will be relatively unfavorable in aluminosilicates, and this effect would be expected to be visible in geopolymers primarily at high x. In the high-x range, the model generally slightly underestimates the level of Q^4(2Al) present, while overestimating Q^4(0Al). However, exact quantification of the Q^4(0Al) peak in the deconvolution procedure was not always straightforward, as this peak is often very small and hence difficult to distinguish from the spectral background, so no great significance should be drawn from the difficulties in model fitting to this peak. In the moderate-x region, the level of Q^4(3Al) is slightly overestimated at the expense of both Q^4(2Al) and Q^4(4Al). This may be related to next-nearest neighbor ordering, or may be related to the nature of the charge-balancing cations, as the deviations from model predictions in this region appear to vary for each Na/(Na+K) ratio investigated.

2.7 USE OF PURE ALUMINOSILICATE SOURCE MATERIALS

Figure 7 shows the ^{17}O 3QMAS NMR spectra of Na- and K-PVA geopolymers with Si/Al ratio of 1.00. The spectra are sheared by a factor of 3, so that the F1 dimension is comprised of only quadrupolar interactions, allowing for more clear separation of linkages based on differences in quadrupolar interactions. The spectrum of K-geopolymer shows clear evidence of all three T-O-T linkages, with the peaks of Al-O-Al and Si-O-Al being overlapped from 0 to –2 kHz, and a small region associated with Si-O-Si centred at –3 kHz. A small peak can be observed in the spectrum at approximately 80 ppm in the F2 dimension, which is currently not assigned. Despite this, the clear observation of Al-O-Al in the K-PVA specimen in Figure 7a provides the first direct evidence of non-Loewenstein Al,Si ordering in geopolymers, though imperfect ordering has been implied from the ^{29}Si MAS NMR investigations described above. The Na-PVA geopolymer in Figure 7b shows similar features to that of the K-PVA specimen, although the degree of disorder is reduced as indicated by the smaller Al-O-Al and Si-O-Si resonances. The reduction in disorder in Na-geopolymer compared with K-geopolymer in Figure 7 correlates extremely well with predictions from the model in Figure 6. In comparison to aluminosilicate glasses (Lee and Stebbins 2000), the poor separation of the different T-O-T linkages implies that the framework structure of geopolymers is highly disordered leading to broad peaks and that the different T-O-T linkages are structurally similar.

Figure 8 presents the XRD diffractograms of the low Si/Al ratio specimens in the current work and the PVA powder with Si/Al ratio of 1.00. It can be observed that the Na-geopolymers with Si/Al ratios close to unity contain a small amount of crystalline material (less than 30% as determined by quantitative XRD using the RIR method). However, the K-PVA specimen is observed to be X-ray amorphous. Therefore, the appearance of the peaks in all specimens with Si/Al ratios close to unity can be assigned to Al-O-Al, rather than structurally distinct oxygen sites in crystalline frameworks. Indeed, the similarity of the NMR peak positions for Na-PVA and K-PVA indicates that the morphology of the bridging oxygen sites in geopolymers is largely independent of alkali cation type. However, the peaks in the K-PVA specimen are observed to be broader, which is both a result of the greater degree of disorder, lack of crystalline phase and the increased quadrupolar interactions in potassium bearing systems. Work on quantification of the ^{17}O 3QMAS-NMR data is ongoing, however preliminary results appear to correspond well to the predictions of the model presented above.

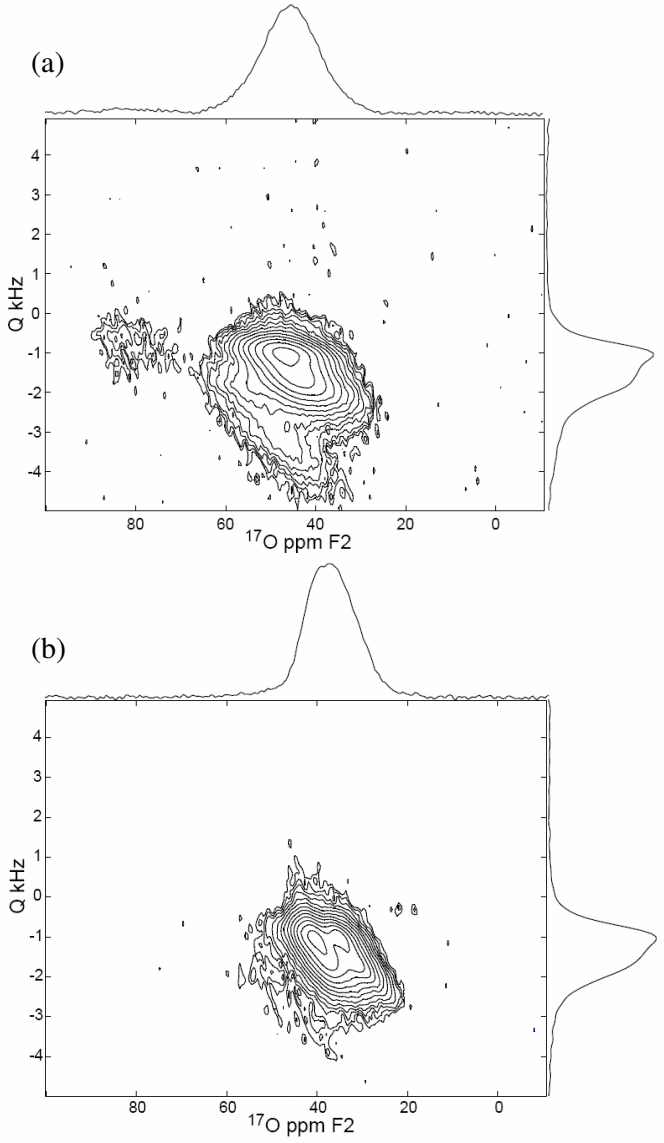

Figure 7. ^{17}O 3QMAS NMR spectra of (a) K- and (b) Na-geopolymer with Si/Al ratio of 1.00. Contour lines show intensity in arbitrary units and are drawn from 1.25% to 99% of highest peak intensity, increasing in multiples of 1.4. Spectra are sheared by a factor of 3 in order to isolate quadrupolar interactions in the F1 dimension.

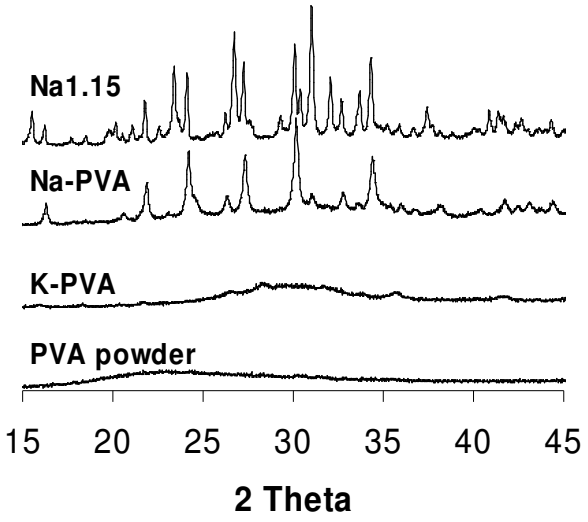

Figure 8. XRD diffractograms of Na1.15, Na-PVA, K-PVA and the PVA powder used in the current work. Peaks in the Na1.15 specimen correlate with faujasite.

Determination of the degree of Al-O-Al avoidance in geopolymers may prove to be important in the analysis of durability and chemical resistance of these materials. It has been noted previously that high-alumina zeolites become structurally weakened by certain cation-exchange processes, which is attributed to breakage of the relatively unstable Al-O-Al bonds (Hass *et al.* 1982). If this is also the case in geopolymers, any attempts to maximize durability or chemical resistance must take into account the degree of Al-O-Al bonding expected. By controlling this through manipulation of synthesis parameters, geopolymers optimized for desired applications may be produced. The results of this investigation suggest that Na geopolymers will inherently have a lesser extent of Al-O-Al formation than K geopolymers, and may therefore be preferable in certain applications. Also, lower synthesis temperatures give a lesser extent of Al-O-Al formation, and should therefore be considered if such properties are desired. These suggestions are yet to be tested experimentally, and the effects of variation in microstructure may be found to swamp the effects of Al-O-Al bond instability. However, considering the significant interest in the use of geopolymers in high-risk applications including immobilization of toxic and/or radioactive wastes, such effects must be taken into consideration.

3. ENERGY-DISPERSIVE X-RAY DIFFRACTOMETRY

This section of the report is based on work accepted for publication as Provis & van Deventer (2006).

3.1 INTRODUCTION

One of the primary advantages of geopolymers over traditional cementitious materials is that correctly-formulated geopolymers are capable of very rapid setting while still attaining high final strengths (Lee and van Deventer 2002). The desire to understand and control this setting behaviour has led to the application of a variety of techniques in the analysis of the early stages of geopolymerisation. In particular, calorimetric and rheological characterisation techniques have provided valuable information regarding the setting process. However, it is difficult to isolate the relative contributions of different steps in the reaction process to the total calorimetric signal, although work in this area is ongoing (Provis *et al.* 2005b), and rheological studies are very difficult once the system has begun to solidify. Environmental scanning electron microscopy (ESEM) has also been used for in situ studies of geopolymerisation (Wei *et al.* 2004), but generally provides a more qualitative view of the process. Ex-situ X-ray diffraction (XRD) studies of geopolymeric 'hydroceramic' materials cured at slightly elevated temperature have used the degree of crystalline zeolite formation as a measure of the extent of reaction (Olanrewaju 2002). However, this technique provides unsatisfactorily low time resolution and relies on the formation of XRD-detectable crystallites, which are not always present in detectable quantities in geopolymers, particularly at higher Si/Al ratios (Provis *et al.* 2005c). It is therefore desirable to develop a technique by which structure development in a setting geopolymer may be directly observed, particularly in terms of isolating the dissolution and reprecipitation steps involved in the geopolymerisation process (van Jaarsveld *et al.* 1997).

The use of in-situ energy-dispersive X-ray diffractometry (EDXRD) using a polychromatic X-ray source and an energy-discriminating detector for rapid obtention of diffractograms was first

suggested in the late 1960s (Giessen and Gordon 1968). However, this technique has only recently become more widely utilised, with recent improvements in synchrotron X-ray sources and detectors providing greatly improved signal-to-noise ratios. Where the standard (angle-dispersive) XRD technique uses a monochromatic beam and a detector that scans through a range of angles, the polychromatic ('white') X-ray beam used in EDXRD allows the energy-discriminating detector to be fixed at a given angle. In Bragg's Law, Eq. (14), the diffracted beams from structures with different d-spacings are distinguished by different values of λ for a fixed θ, rather than the different values of θ observed in standard XRD (using fixed λ).

$$n\lambda = 2d \sin\theta \tag{14}$$

EDXRD has been used particularly in the investigation of hydrothermal reaction processes, which require sample vessels capable of withstanding relatively aggressive environments. The higher penetrating power of the white X-ray beam used in EDXRD compared to a beam that has passed through a crystal monochromator (required for standard, angle-dispersive XRD experiments) enables the use of 'laboratory-sized' sample cells in transmission geometry, thereby greatly simplifying experimental design and expanding the available parameter space. The removal of the need to scan the detector across a range of angles also greatly decreases the collection time required to obtain a diffractogram. Some spatial resolution is sacrificed due to the difficulties inherent in energy-discriminating detectors, meaning that diffraction data obtained by EDXRD is most likely unsuitable for use in a structure refinement, but the temporal resolution achievable more than compensates for this.

The primary purpose of the work reported here is to outline the value of EDXRD as a technique for the study of the kinetics of geopolymerisation. A series of potassium aluminosilicate geopolymers of varying Si/Al ratio are synthesised within a purpose-designed sample cell, and the reaction kinetics observed by EDXRD. It is shown that EDXRD provides sufficient time resolution to distinguish certain important features of the reaction process, and therefore provides a valuable complement to more established techniques.

3.2 EXPERIMENTAL METHODS

Experiments were conducted at beamline X17C of the National Synchrotron Light Source (NSLS), Brookhaven National Laboratory, NY. This is a superconducting wiggler beamline, providing sufficient X-ray flux for experiments to be conducted in transmission geometry using a relatively large (approx. $2cm^3$) sample. The beam size was 25×12μm. A purpose-built sample vessel, constructed from stainless steel with a thin PTFE insert and end caps to contain the sample as shown in Figure 9, was mounted on a kinematic stage and inserted into the beamline.

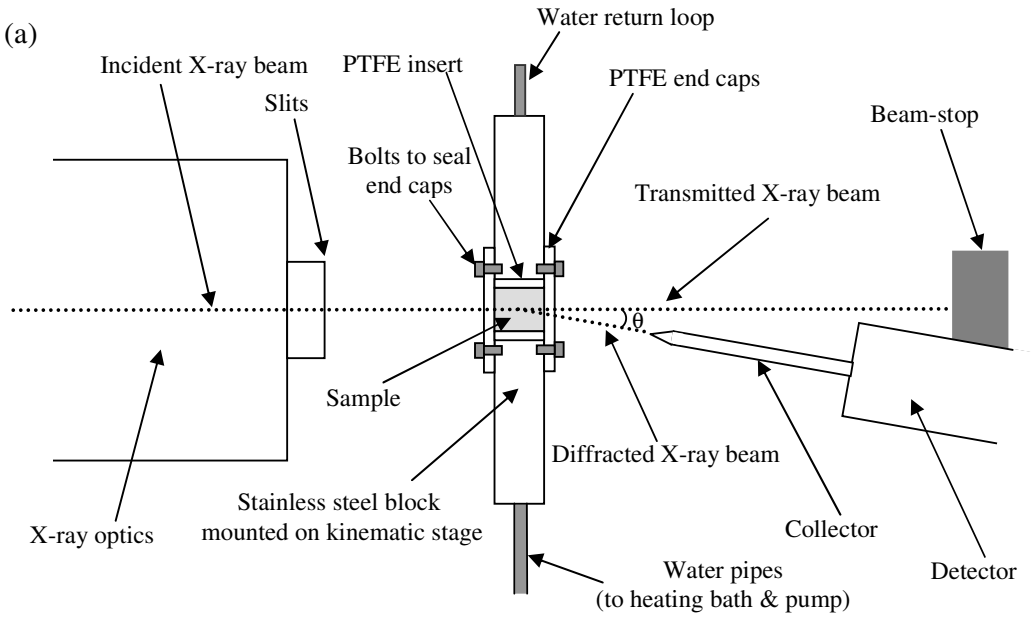

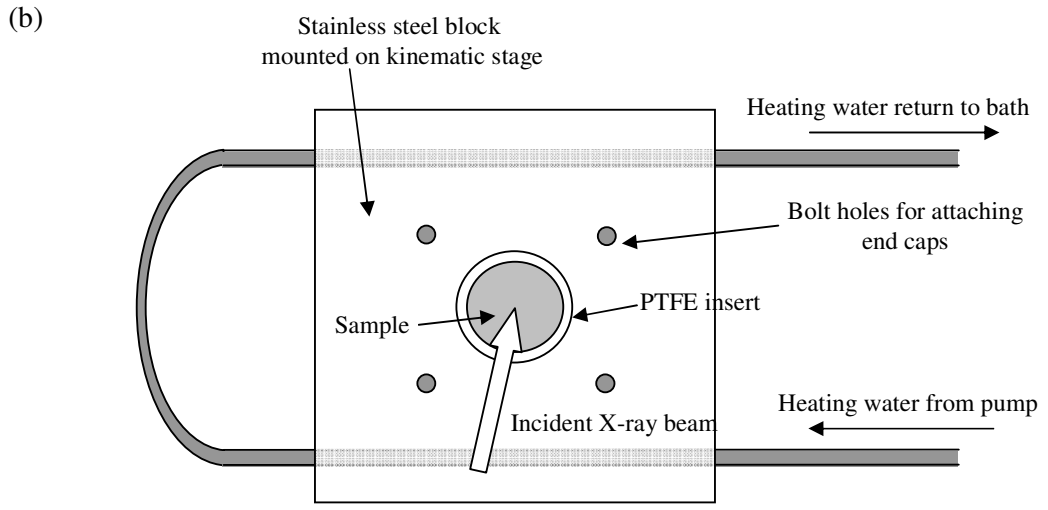

Figure 9. Schematic diagrams of the experimental apparatus: (a) top cutaway view, not to scale, (b) front view of reaction cell with PTFE end cap removed.

Temperature control in the reaction cell was achieved via the heating loop depicted in Figure 9, with water from a temperature-controlled bath circulated by a small pump through channels drilled in the stainless steel block. The reaction cell temperature was able to be controlled to within approximately ± 3°C (at 40°C) using this system. The time taken to reach the desired reaction temperature (40°C) following filling of the cell with geopolymer paste and connection of the heating system was less than the time taken to mount the cell on the kinematic stage and carry out the required safety procedures prior to the start of data collection. Therefore, temperature variation during start-up of the experiments is not considered in detail in this investigation, although it will be discussed later as a possible source of error.

X-ray detection and energy discrimination was achieved by the use of a solid-state Ge detector, located at a fixed 2θ angle of 8°, utilising a 0.3×1.0mm brass collector and analysed through a 4000-channel MCA, spanning the energy range 3-74 keV. Calibration was carried out using a polycrystalline gold standard. The volume sampled by the X-ray beam was much smaller than the actual geopolymer paste volume, which meant that exact sample alignment was much less critical than in most beamline-based experiments. This was essential in ensuring the shortest possible start-up time for each experiment, allowing the maximum possible amount of data to be collected

in the early stages of reaction. The 3D kinematic stage was set in the appropriate position, which remained constant throughout the series of experimental runs. Once the sample chamber was filled and the temperature control system attached, the vessel was mounted on the stage using a G-clamp. Measurements taken using a dummy sample with the kinematic stage located in a variety of different positions (much wider than the variability allowed in the start-up procedure for the actual experiments) all produced identical results. Therefore, any slight variations in sample position due to the abbreviated sample alignment procedure will not have any effect on the results obtained.

Potassium silicate solutions were prepared by dissolving amorphous silica in KOH solution with H_2O/K_2O = 11.0, giving solutions with composition SiO_2/K_2O = 0.0, 1.0, and 2.0. These solutions were then each mixed with stoichiometric amounts of metakaolin (MetaMax EF, Engelhard, NJ, USA, SiO_2/Al_2O_3 = 2.0) using a high-speed mechanical mixer to give smooth geopolymer pastes with K_2O/Al_2O_3 = 1.0 and SiO_2/Al_2O_3 ratios of 2.0, 3.0 and 4.0 respectively. A quantity of the paste was then transferred to the reaction cell, which was sealed, attached to the heating system and mounted on the kinematic stage in the beamline. The time taken from the start of mixing to the start of data collection was recorded for each experimental run, and was always in the range 7-9 minutes. The exact time taken to load the sample was dependent on the SiO_2/K_2O ratio of the geopolymer, as the higher-SiO_2 activating solutions are very viscous and therefore require more mixing time to produce a homogeneous geopolymer paste.

3.3 NOTES ON DATA COLLECTION AND PROCESSING

In selecting the collection time for an in situ EDXRD experiment, a compromise must be drawn between maximising the signal to noise ratio of each data set (energy resolution) and maximising the number of data sets collected (temporal resolution). Given that the main purpose of this investigation was the study of the kinetics of geopolymerisation, and that metakaolin-based geopolymers generally show no sharp diffraction peaks (Provis *et al.* 2005c), a collection time of approximately 150s was selected as being appropriate. Use of a collection time this short allows the obtention of a sufficient number of data points in the early stages of reaction. The spectrum obtained at each point in time was then smoothed by averaging over blocks of 7 adjacent energy channels, which significantly reduced the noise in the data without sacrificing any valuable

information due to the very broad nature of all peaks being observed. Figure 10 shows a comparison between the raw and smoothed data sets obtained after 60 minutes of reaction

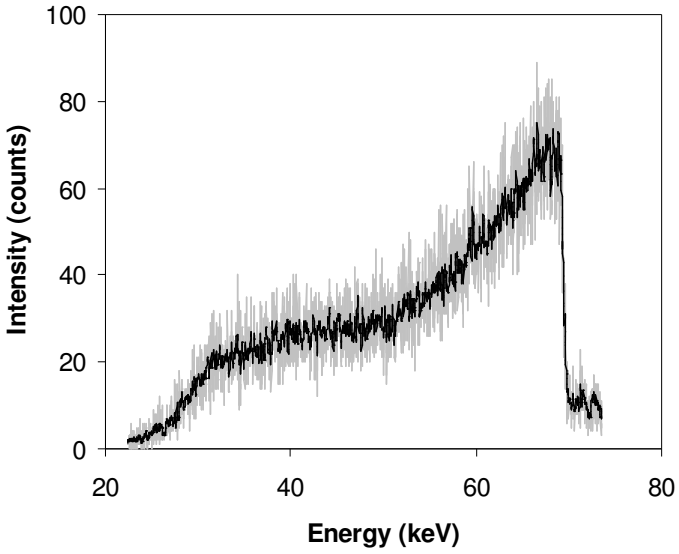

Figure 10. Effects of smoothing over 7 adjacent energy channels: Spectrum obtained from sample with SiO_2/Al_2O_3 = 3.0 after 60 minutes of reaction at 40°C, raw (gray line) and smoothed (black line).

For the purposes of comparison between data sets, all values used in quantitative analysis are normalised by dividing by the total intensity (area under the curve). This is necessary due to fluctuations in beam intensity during a kinetic run, and removes the need to correct separately for detector deadtime effects.

3.4. RESULTS AND DISCUSSION

Figure 9 shows smoothed and normalised data sets for the geopolymerisation of pastes with SiO_2/Al_2O_3 = 2.0, and comparable results are obtained for other compositions. Each data set shown was collected over a 150 second period.

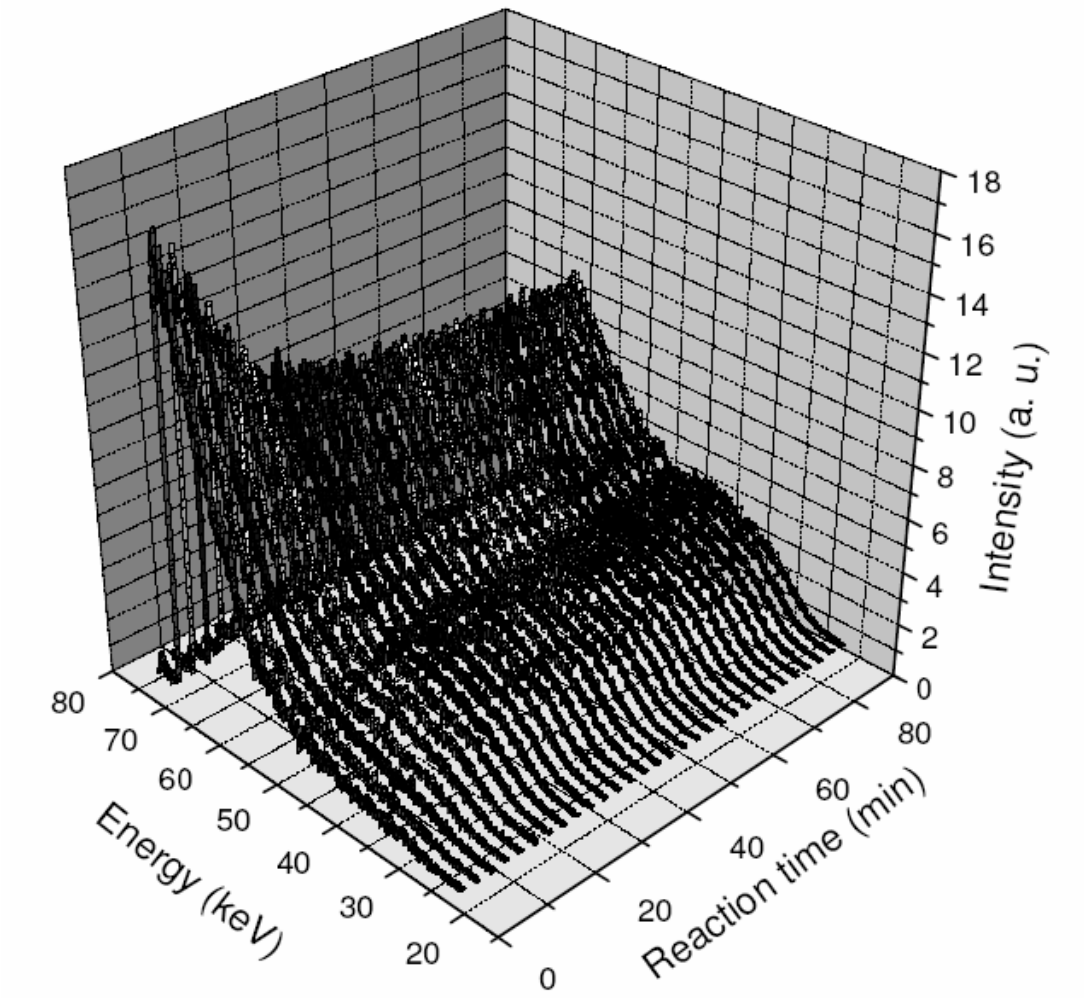

Figure 11. Smoothed and normalised EDXRD data for the system with $SiO_2/Al_2O_3 = 2.0$.

All data sets show a superficially similar trend in reaction progress across compositions. Each set of diffractograms shows a large feature at high energy (~68 keV) in the initial stages of the reaction, which gradually diminishes and is replaced by a broad peak at ~30-50 keV as the reaction progresses. It is not yet entirely clear which structural features of the geopolymerising paste are responsible for these features, particularly given that the high-energy peak corresponds to a d-spacing of around 1.3Å, which is significantly shorter than the T-O bond length (~1.6Å, T: tetrahedral Si or Al). However, it is possible that this peak is at least partially due to scattering from small dissolved species, which would explain why its relative intensity decreases with the solidification of the reacting paste.

The rapid decrease in spectral intensity below 30 keV is due to absorption effects. X-rays below this energy cannot pass through a sample and vessel endcaps as thick as those used here, rendering any effects at d-spacings greater than approximately 3.0Å unobservable. The design of the X17C beamline and detector also do not allow the use of a smaller 2θ angle which would render longer d-spacings accessible. It is hoped that future work, possibly in further reducing the sample vessel size and endcap thickness to minimise absorption while maintaining the rapid initialisation capabilities of the current apparatus, will lead to improvements in this area.

Quantification of the extent of reaction based on EDXRD data was achieved based on the simple assumption that each intermediate spectrum was able to be represented as a linear combination of the first and last spectra obtained. The data presented represent the time period from the start of reaction until the reaction had slowed sufficiently that no change was observable for several successive spectra. Once these data had been collected, a spectrum with a much longer (usually 2000s) collection time was obtained, to provide a 'final' reference point with the highest possible signal to noise ratio. Fitting each intermediate spectrum according to Equation (15) by a least-squares error minimisation gave a respectably accurate fit to the spectra.

$$(\text{Spectrum at time } t) = x(\text{Final spectrum}) + (1-x)(\text{Initial spectrum}) \qquad (15)$$

However, it must be noted that the raw x values obtained by this procedure are not in fact a truly representative measure of the extent of reaction at any given point in time, due to the fact that the first data point could not be obtained at time $t = 0$. To remedy this, some means of estimating the extent of reaction during the period leading up to the obtention of the first spectrum is necessary. It was initially hoped that it would be possible to use the spectrum of unreacted metakaolin as a point of comparison to obtain this information. However, differences in X-ray absorption behaviour between metakaolin and the geopolymer pastes due to their different atomic compositions cause severe complications in this procedure. Therefore, a simpler method for estimating the rate of reaction in the initial stages of geopolymerisation was chosen. It was observed from the data sets presented in Figure 9, as well as others not shown here, that the extent of reaction in the early stages of geopolymerisation, to a first approximation, increases linearly. This observation was used to provide an estimate of the progress of the reaction in the time period leading up to collection of the first spectrum, and appears to give results that are reasonably accurate. Future work is intended to provide a better solution to this problem, both

with respect to design of apparatus and experiments and also in numerical treatment of experimental data.

Having corrected the raw data obtained by spectral fitting using this assumption of linearity, Figure 12 is obtained. This figure shows that the primary aim of this investigation, to develop an accurate means of quantifying the rate of the initial stages of geopolymerisation using EDXRD, has been achieved. The trend shown in Figure 12, where the rate of reaction decreases with increasing SiO_2/Al_2O_3 ratio for samples of constant H_2O/K_2O ratio, corresponds to previous observations using calorimetric and rheological techniques (Rahier *et al.* 1997; van Jaarsveld and van Deventer 1999).

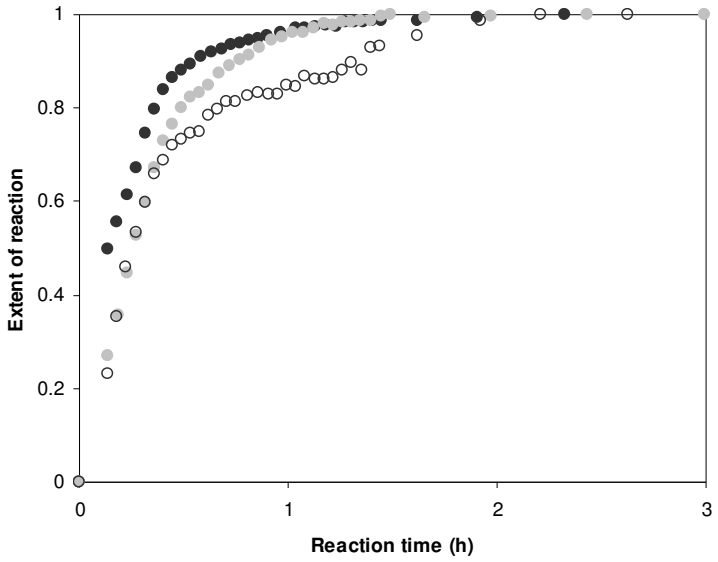

Figure 12. Plot of extent of reaction vs time for samples with SiO_2/Al_2O_3 = 2.0 (black circles), 3.0 (grey circles) and 4.0 (unfilled circles).

Figure 12 shows that increasing the SiO_2/Al_2O_3 ratio of a geopolymer paste reduces the rate of the initial burst of reaction prior to solidification of the paste. It is not currently possible to quantify the total proportion of metakaolin converted into geopolymeric binder by EDXRD. However, ^{27}Al MAS-NMR has shown that the total extent of conversion of metakaolin into geopolymer after curing for 2 weeks decreases with increasing SiO_2/Al_2O_3 ratio (Duxson *et al.* 2005b). The results presented here provide a potential explanation for this trend, in that the slow

initial rate of reaction in very high-silica systems may mean that these pastes solidify before the dissolution of metakaolin reaches completion. The apparent 'step' in the SiO_2/Al_2O_3 =4.0 data set in Figure 12 after approximately 1 hour of reaction provides further evidence for this suggestion, as it appears that the reaction becomes drastically slower at this point, which corresponds to a relative extent of reaction of around 0.8. Approximately 20% of the reaction observed occurs after this point in time, but it is likely that metakaolin dissolution will be greatly hindered by the reduced mobility of the dissolved species following solidification. Therefore, the lower overall extent of metakaolin conversion in these systems is not unexpected. This is in contrast to the lower-silica samples (SiO_2/Al_2O_3 = 2.0 and 3.0), where Figure 12 shows that the reaction goes essentially to completion in the first 90 minutes after mixing.

4. KINETIC MODELLING OF GEOPOLYMERISATION

This section is an abbreviated version of Chapter 8 of the Ph.D. thesis of John L. Provis, submitted for examination at the University of Melbourne, 28 March 2006.

4.1. INTRODUCTION

Previous studies of the kinetics of geopolymerisation have generally focussed on the application of different experimental techniques – primarily calorimetry – to obtain a largely empirical understanding of geopolymer setting rates. The research program led by Palomo has studied the effect of various parameters including reaction temperature and calcium addition via isothermal conduction calorimetry (ICC) (Granizo *et al.* 2000; Alonso and Palomo 2001a; b). Rahier and colleagues pioneered the use of quasi-isothermal modulated differential scanning calorimetry (DSC) as a means of simultaneously observing changes in heat flow and heat capacity during geopolymeric setting, and coupled these measurements with rheological data (Rahier *et al.* 1996a; 2003). Both groups provided links between heat release data and the final mechanical strength of the geopolymeric products, however little or no analysis of the underlying causes of the observed trends in the heat flow signals was undertaken. In particular, it is clear from the multiple heat flow peaks observed during geopolymerisation that there are multiple chemical steps occurring, however the most detailed analysis of this presented in the literature is a comment by Rahier *et al.* (2003) that the reaction appears to have at least two steps – dissolution and polymerisation – and that the second step 'seems to be autocatalytic.'

Given the relative paucity of data regarding the kinetics of geopolymerisation, it is therefore necessary to look further afield to obtain a starting point for an investigation such as this. Faimon (1996) developed a reaction kinetic model as a means of understanding oscillations in dissolved species concentrations during leaching, and provides a means of analysing both dissolution and reprecipitation steps within an overall reaction process. This model is outlined in Figure 13. The most notable feature of the Faimon model is the autocatalytic step whereby the oligomeric

aluminosilicate species combine to form polymers. This is very reminiscent of the observation of autocatalysis in the DSC experiments of Rahier *et al.* (2003), and suggests some potential applicability of this model, in modified form, to the study of geopolymerisation.

4.2 EXTENDING THE FAIMON MODEL

By extension of the model of Faimon (1996), the process of geopolymerisation may be described from a reaction kinetic standpoint. The obvious differences between geopolymerisation and the processes described by the original Faimon model are that the aluminosilicate 'minerals' in geopolymerisation are in fact metastable and/or pozzolanic materials such as metakaolin or fly ash, and that the pH of a geopolymer reaction slurry is two or more units higher than is used to study mineral weathering. The net effect of these differences is twofold: (1) the geopolymerisation reaction will be largely completed on a much shorter timescale than those on which aluminosilicate weathering is observed; and (2) the products of the reaction should include both gel and zeolitic phases as was discussed in detail earlier.

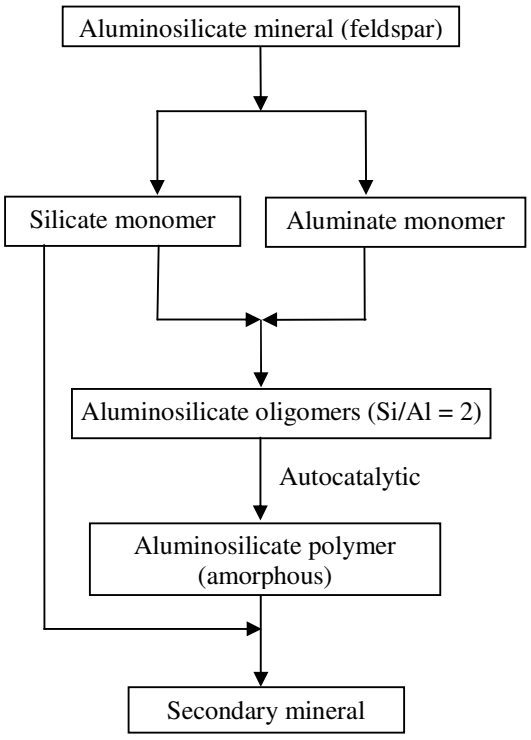

Figure 13. The aluminosilicate weathering model of Faimon (1996).

The model of Faimon (1996) as shown in Figure 13 allows for dissolution of a primary mineral into aluminate and silicate monomers, association of these monomers via both addition and autocatalytic polymerisation routes, and formation of an unidentified 'secondary mineral' phase. Its extension to geopolymerisation (Figure 14) is therefore relatively straightforward, requiring only:

- Incorporation of the effect of silicate oligomerisation (species D) in the concentrated activator solutions

- Deviation of oligomer (species O) stoichiometry from 2:1 to account for the range of Si/Al ratios with which geopolymers may be synthesised,

- Identification of the secondary mineral product G as the amorphous aluminosilicate gel component of the geopolymeric binder, and

- Inclusion of a second reaction pathway by which the zeolitic phases (N and Z) observed in geopolymers are formed. Species Z is designated to be slightly higher in Al than its amorphous counterparts, following the observation that the crystalline products of hydrothermal zeolite synthesis tend to be enriched in Al compared to their amorphous (gel or fly ash) precursors, and to the system as a whole (Barrer and White 1952; Ogura *et al.* 2003; Tanaka *et al.* 2004; Yang *et al.* 2004).

Including these effects into the model then gives Figure 14; a flowsheet outlining the reaction kinetic model for geopolymerisation proposed here. An additional reaction, shown as a grey arrow in Figure 14, shows the conversion of gel to zeolite over an extended curing period (Duxson *et al.* 2006). However, as the primary focus of the reaction kinetic model is on the initial stages of the reaction, the gel/zeolite interconversion process will not be incorporated into the model formulation.

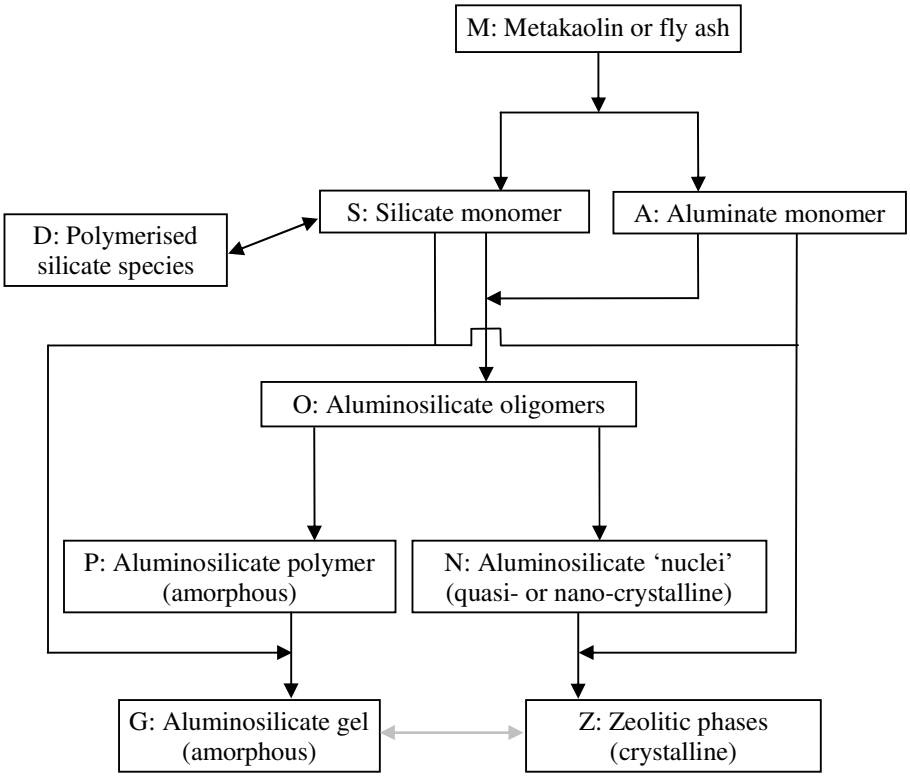

Figure 14. The proposed reaction sequence of geopolymerisation.

To ensure reasonable calculation times for the reaction kinetic model, simple expressions were used to represent the fraction of the dissolved silicate present as monomers and the average polycondensation of species D (denoted n_D). These expressions were obtained by fitting a simple quadratic function to percentage monomer and average polycondensation data obtained from the ^{29}Si NMR data of Provis *et al.* (2005d), and are presented in detail by Provis (2006).

4.3 Model formulation and justification

The reactions postulated to be involved in the formation of geopolymers from a solid aluminosilicate source (metakaolin or fly ash) and sodium hydroxide or silicate solution, and the kinetic expressions used to describe these reactions, are outlined in Table 2, with kinetic parameters given in Table 3.

Table 2. Reactions modelled, with corresponding kinetic expressions. Abbreviations correspond to species defined in Figure 14, with W representing one mole of water. Deprotonation effects are neglected.

	Reaction	ΔH_r (kJ/mol)	Rate expression	Comment
(1)	$M + 4W \rightarrow 2x_M S + 2(1-x_M)A$	-134.3 [a,b]	$r_1 = k_1 M$	Metakaolin $x_M = 0.500$
		-35.1 [b,c]	$r_1 = k_1 MA^{-0.35}$ [d]	Gladstone fly ash $x_M = 0.661$ [e]
(2)	$A + nS \rightarrow O + (n+1)W$	$-190.2 \times n$ [f]	$r_2 = k_2 AS^n$	
(3)	$n_D S \leftrightarrow D + n_D W$	$-41.8 \times n_D$ [f]	(equilibrium)	
(4)	$2O \rightarrow P + (n_O+1)W$	$-37.05 \times (n_O + 1)$ [f]	$r_4 = k_4 O^2$	
(5)	$2P + 2O \rightarrow 3P + (n_O+1)W$	$-37.05 \times (n_O + 1)$ [f]	$R_5 = k_5 P^2 O^2$ [g]	
(6)	$2O \rightarrow N + (n_O+1)W$	$-37.05 \times (n_O + 1)$ [f]	$r_6 = k_6 O^2$	
(7)	$N + S + A \rightarrow Z + (n_N+5)W$	$-2.1 \times (2n_N + 4)$ [h]	$r_7 = k_7 NSA$	
(8)	$P + S \rightarrow G + (n_P+3)W$	$-2.1 \times (2n_P + 4)$ [h]	$r_8 = k_8 PS$	

[a] Vaughan (1955)

[b] Wagman *et al.* (1968)

[c] Navrotsky and Tian (2001)

[d] Oelkers and Gislason (2001)

[e] Sindhunata (2006)

[f] Catlow *et al.* (1996)

[g] Faimon (1996)

[h] Yang *et al.* (2000)

Here, x_M is the Si/(Si+Al) ratio of the reactive aluminosilicate source material, and n_k (k = O, N, P) is the Si/Al ratio of species k. The value n is defined as S/A, the ratio of monomeric silicate to aluminate in solution. Fly ashes consist of a mixture of glassy and crystalline phases, of which the glassy phases tend to be significantly more reactive (Diamond 1986). Over the short timescales on which geopolymeric setting occurs, these phases are expected to be the predominant source of dissolved aluminosilicate species, and so the description of fly ash dissolution during geopolymerisation will follow the rate laws previously observed by Oelkers and Gislason (2001) for aluminosilicate glass dissolution under alkaline conditions.

Table 3. Values of parameters defined in Table 8.2. Units of rate coefficients are arbitrary, and rate coefficients are modified by multiplying by a factor related to the system water content as described below.

Rate coefficients	
k_1 (fly ash)	4.1×10^{-5} × (monomer fraction)
k_1 (metakaolin)	6.0×10^{-4} × (monomer fraction)
k_2	1.0×10^{-2}
k_4	8.0×10^{-5}
k_5	5.0×10^{-2}
k_6	6.0×10^{-4}
k_7	1.0×10^{-5}
k_8	3.0×10^{-5}
Time scale parameters ($t_{real} = t_{model}/\tau$)	
Fly ash, 50°C	4.0×10^{5} h^{-1}
Metakaolin (MetaMax EF), 40°C	5.0×10^{3} h^{-1}

The heat of reaction data and rate expressions shown in Table 2 do require some additional explanation:

- As was noted earlier, it is believed that the most highly reactive phases in fly ashes are glassy. Sindhunata (2006) conducted quantitative XRD and XRF studies of the Gladstone fly ash used in the experiments to be modelled here, and found it to contain 17.0% and 39.1% amorphous Al_2O_3 and amorphous SiO_2 respectively, with Ca and Fe impurities. Navrotsky and Tian (2001) found that the enthalpy of formation from crystalline oxides of a calcium aluminosilicate glass of composition $Ca_{0.167}Al_{0.333}Si_{0.667}O_2$ is 0.37 ± 0.31 kJ/mol. Given that this is very close to zero, and that data were not available for comparable Fe-containing systems, the enthalpy of formation of the reactive phase in fly ash was taken to be equivalent to that of a mixture of α-Al_2O_3 and quartz, with the same Si/Al ratio as the glass. On this basis, the value shown in Table 8.2 was obtained.

- The kinetic expression for each reaction step is developed from the assumption that the stoichiometry of the reaction predicts the kinetics. This is not to suggest that these steps are in fact elementary reaction steps, as it is clear from the stoichiometry of the reactions that this is not the case. However, in the absence of any alternative

information regarding the order of each reaction, this assumption has been found to give a reasonably accurate prediction of the kinetics of the reactions occurring during geopolymerisation. The exception to this is in the case of reaction 1 for fly ash, where it is known that the dissolution of an aluminosilicate glass of very similar stoichiometry to the Gladstone fly ash used here has a -0.35 power dependence on dissolved $Al(OH)_4^-$ concentration (Oelkers and Gislason 2001). This information is incorporated into the rate expression. Also, a simple first-order dependence on aluminosilicate source material content is used rather than attempting to describe the surface-controlled dissolution processes.

- The stoichiometry and rate expression for the autocatalytic reaction (reaction 6) are taken directly from the model of Faimon (1996).

- The ΔH_r data for reactions 2-6 were obtained from the ab initio/molecular mechanics calculations of Catlow *et al.* (1996), who calculated the heats of reaction between a variety of small solvated silicate, aluminate and aluminosilicate species. In each case, the value shown in Table 8.2 is the heat released by bond formation, multiplied by the number of bonds formed in each reaction.

- The heats of formation (per mole TO_2, T = Si or Al) of species Z and G from their respective precursors N and P were assumed to be equal, with the enthalpy of crystallisation of faujasite from an amorphous precursor (Yang *et al.* 2000) selected as an appropriate value. Multiplication by the number of T-atoms from the definition of each species then gives the ΔH_r values as shown.

- The values k_1-k_8 are empirically determined rate coefficients. k_4 is small, as species P is primarily formed via the autocatalytic route with rate coefficient k_5 (Faimon 1996). However, a reservoir of species P is required for autocatalysis to commence, and so a small non-zero value of k_4 describes the formation of species P by routes other than the autocatalytic pathway.

- The participation of water in the reaction scheme is modelled by a modifying factor in the rate constant of each reaction in which water is involved. The water content of the system is calculated at every timestep.

- The dissolution rate of the glassy phases in the fly ash and of the metakaolin will also depend highly significantly on the system pH. Therefore, the relationship developed for the fraction of silicate present as monomers is used as a proxy for the pH dependence of the dissolution rate. Throughout the reaction process, k_1 is modified by being multiplied by the fraction of silicate present as monomers, which provides at least an estimate of the pH dependence of the dissolution reaction.

4.4. MODEL APPLICATION

Figure 15 shows a comparison of model predicted heat flow to the observed heat flow in the early stages of geopolymerisation of fly ash, as measured by Sindhunata (2006) using ICC. A baseline of 5 J/g.h was subtracted from the experimental data, and the model predictions are offset by 0.15 h to account for the time taken to load and initialise the calorimeter.

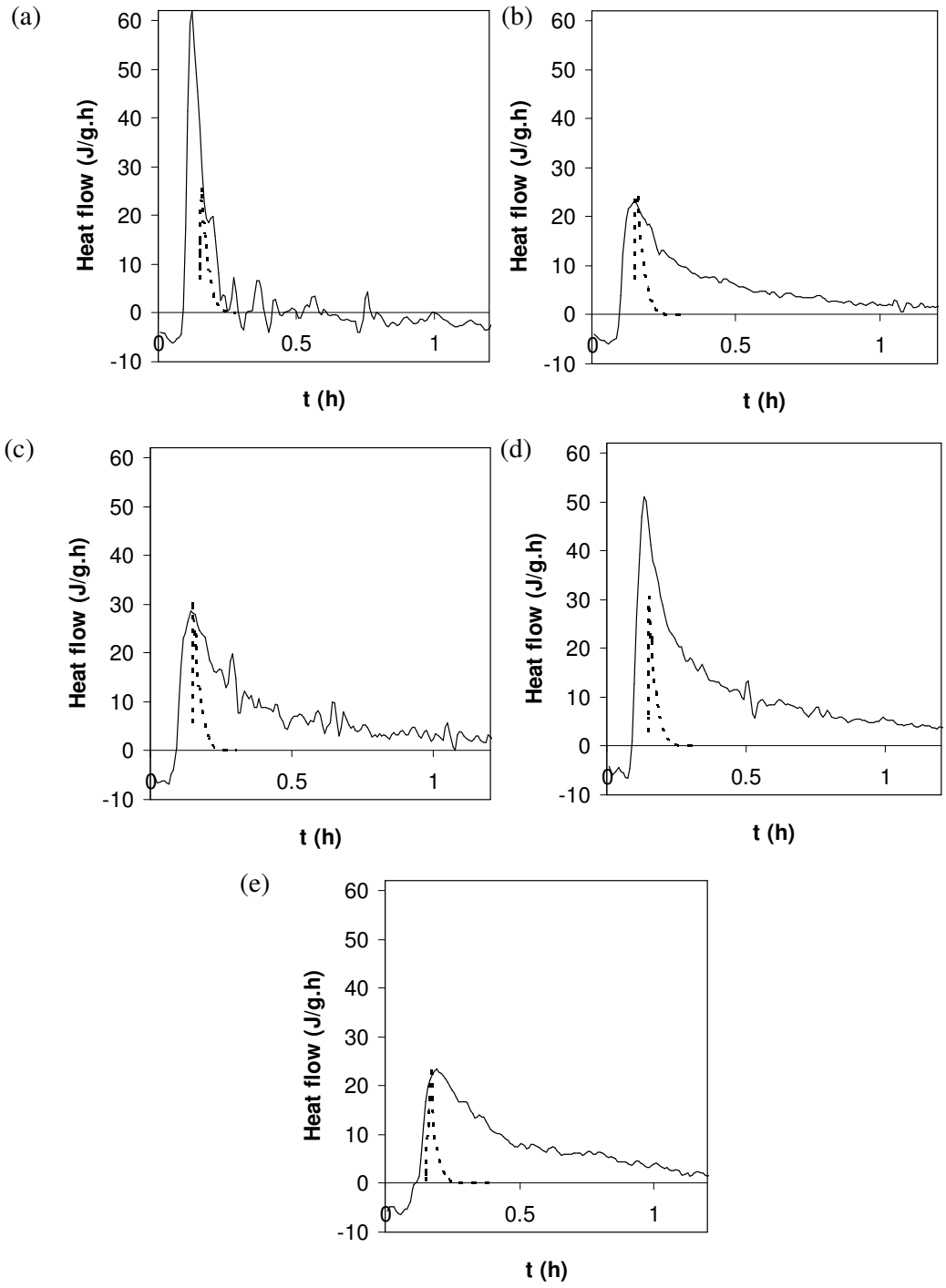

Figure 15. Comparison of predicted heat flow (dashed lines) during geopolymeric setting to experimental ICC data of Sindhunata (2006) (solid lines) for Gladstone fly ash activated with sodium silicate solutions with SiO_2/Na_2O ratios of (a) 0.0, (b) 0.20, (c) 0.50, (d) 0.79 and (e) 2.0. Reaction temperature in all cases was 50°C, with reaction mix composition Na_2O/(reactive Al_2O_3) = 1.11, H_2O/Na_2O = 14.85.

From the graphs in Figure 15, it may be observed that the model predictions fit satisfactorily the trends in the experimental data. The fact that the exact sizes and positions of the heat flow peaks do not precisely match the experimental data is of only minor concern, as the ability to predict trends in such data is realistically all that can be expected from a simplified empirical model. The trend in heat evolution behaviour with changing silica content is thus represented well by the variable-stoichiometry model as proposed.

The EDXRD data presented here provide a second means of experimental validation of the model results. Figure 16(a) shows the relative rates of reaction in K-geopolymer systems as a function of SiO_2/Al_2O_3 ratio, and Figure 16(b) shows the corresponding model predictions. The extent of geopolymerisation in the model is calculated as the ratio $\frac{P+G+N+Z}{M+P+G+N+Z}$, being the fraction of the total "solids" content (defining "solids" as Q^3 coordination or higher) that has reacted.

From Figure 16, it is seen that the model is again able to relatively accurately predict the trends in reaction extent as a function of activating solution silica content. The model predicts a limited effect of silica addition in silica-poor compositions, moving towards a significant effect at the high-silica end of the composition range. Without detailed description of gelation and its effects in hindering mass transport during setting, the minimum in reaction rate at SiO_2/Al_2O_3 is unable to be reproduced, however this is not of significant concern given the significant additional complexity that would have to be introduced into the model if hindered mass transport were to be described accurately. Essentially, the model as it stands assumes chemical reaction control of all processes, and a change-over to mass transport control upon gelation would require either application of an empirical correction term, which is not considered desirable, or fundamental changes to the model structure during the reaction process. This may be the focus of future investigations in this field, but is beyond the scope of the current work.

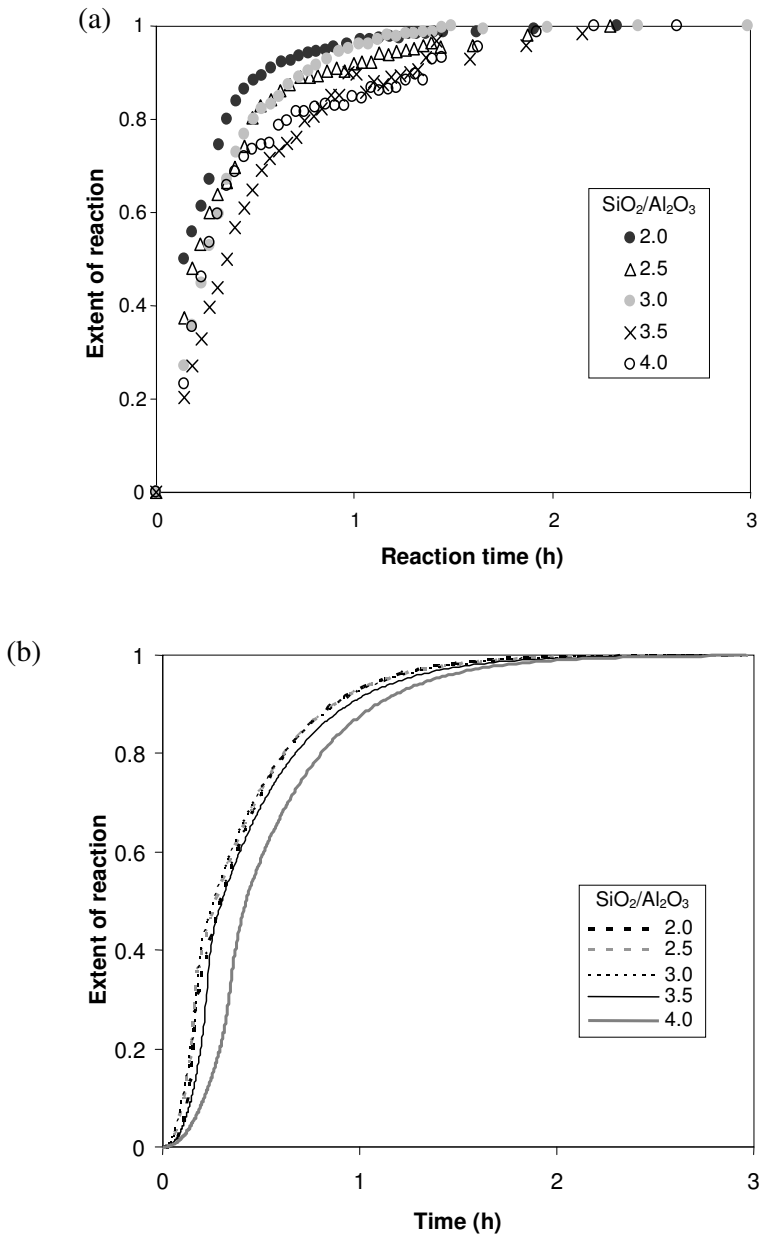

Figure 16. Comparison of (a) experimental EDXRD data and (b) model predictions for the rate of geopolymerisation for K-geopolymer systems with SiO_2/Al_2O_3 ratios as shown.

Figure 17 shows the fraction of T-sites present in each model species and the variation of n, n_O, n_P, n_G, n_N and n_Z with time, for the reaction of Gladstone fly ash with an activating solution SiO_2/Na_2O ratio of 0.79.

(a)

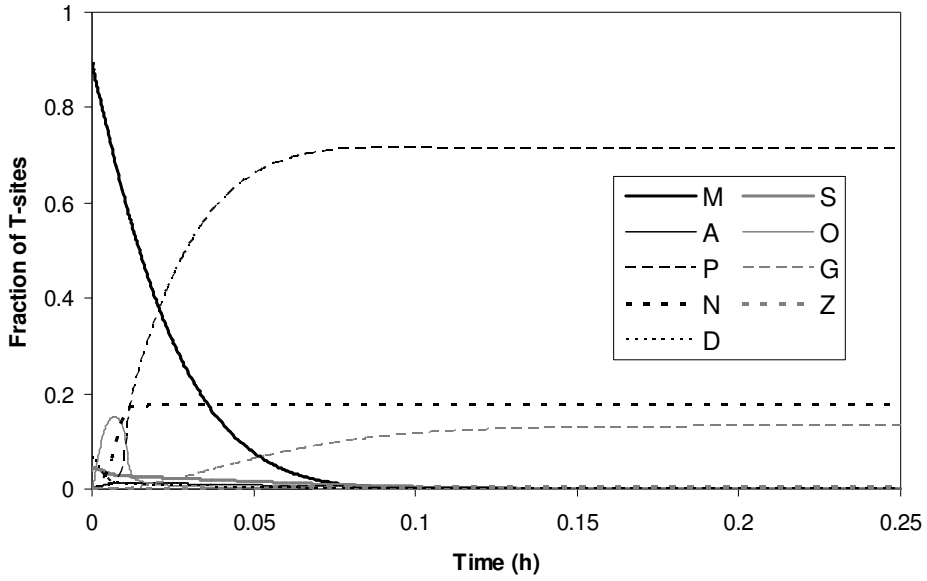
Fraction of T-sites
Time (h)
M
S
A
O
P
G
N
Z
D

(b)

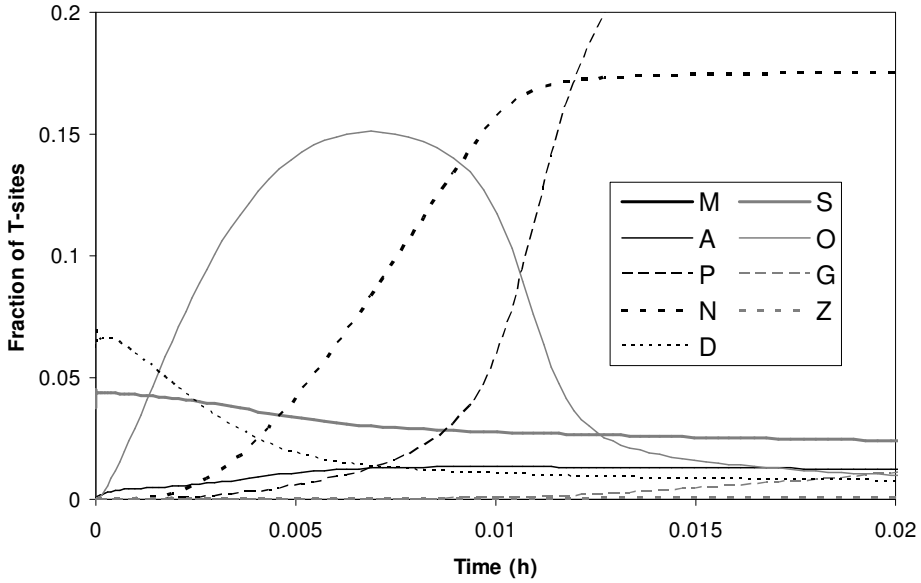
Fraction of T-sites
Time (h)
M
S
A
O
P
G
N
Z
D

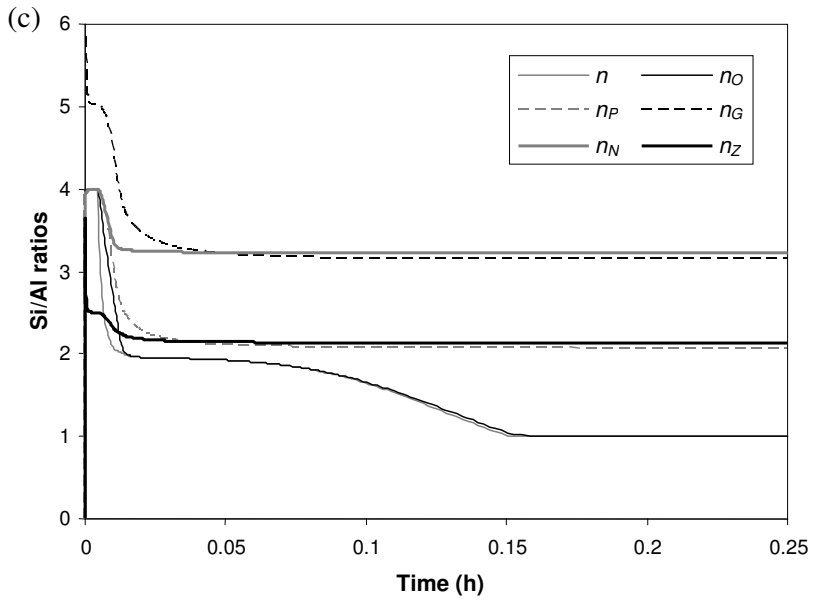

Figure 17. Model reaction progress data for the Gladstone fly ash – sodium silicate system with activating solution SiO_2/Na_2O = 0.79: (a) Fraction of T-sites present within each model species, (b) Expanded view of the bottom left-hand corner of (a), and (c) the variation in Si/Al ratios of each of the species with time.

Figure 17 shows that the progress of the reaction in this system is initially very rapid, but slows significantly following the initial burst of autocatalytic polymerisation. The primary geopolymeric phases formed at this composition are initially P and N, with G increasing significantly at a slightly later time. The formation of G depletes S and D from the solution, which then limits the further formation of G and also crystallisation of N to form Z. In a real geopolymerisation system, there will be some degree of reversibility in the condensation reactions (Provis 2006), and so the reaction will gradually progress to completion. The Si/Al ratio of each species decreases from an initial high value due to the presence of a moderately high-silica activating solution and very low initial dissolved alumina levels. When activating an aluminosilicate source with a silicate-free solution, this situation is reversed with an initial low Si/Al ratio in most species initially increasing rapidly then stabilising.

Figure 17b shows that the reactions of species O to form N and P are relatively slow initially. However, once sufficient P is present for the autocatalytic reaction to start, O is depleted rapidly and P forms in preference to N. The continual dissolution of the fly ash provides a course of S and A, which are each present in small but significant quantities at this point of the reaction, and

appear to remain almost at a quasi-steady state for at least part of the reaction period, with the rates of their depletion and generation approximately equal.

4.5. ADVANTAGES AND LIMITATIONS OF THE MODEL

It must be noted that the formulation presented here represents a relatively preliminary stage in the development of a mathematical description of geopolymerisation, with the aim of outlining the potential for the uses of modelling in analysis of geopolymerisation rather than attempting to show a fully-fledged all-encompassing description of this process. Further model development should be undertaken based on a broader set of experimental data, utilising a wider range of system compositions and various different experimental techniques including in-situ FTIR and NMR modelling of reaction processes, as well as the further use of model systems similar to the to isolate and analyse aspects of the overall process. For example, mass transport, and therefore nucleation and crystal growth, will become increasingly hindered as gelation occurs. Possible non-stoichiometric dissolution phenomena must be accounted for, particularly in the extension of the model to deal with heterogeneous aluminosilicate sources such as fly ash. A full description of the kinetics of geopolymerisation should describe such effects on a fundamental level, but the current level of understanding of geopolymerisation by experimental techniques is not sufficient to allow accurate analysis even by empirical methods, let alone fundamentally-based description. In particular, the differing sizes, compositions and reactivities of the particles present within a particular sample of fly ash have a significant effect on the geopolymerisation process, and this will need to be reflected in the model if its full utilisation in commercially valuable fly ash-based systems is to succeed.

As an illustration of the potential insight the application of mathematical techniques brings to the study of geopolymerisation, even the relatively simplified model presented here provides a significant measure of understanding of this complicated process. The factors identified during model formulation as being critical to the kinetics of geopolymerisation, in particular the rate of dissolution of the solid aluminosilicate source, the rate of nucleation of solid phases and the distribution of silicate species of varying sizes, are now able to be analysed further. Both experimental and computational techniques must be used side-by-side in this analysis to

maximise the information obtainable, which will allow further development of geopolymer technology and its use in a much broader range of applications.

5. CONCLUSIONS

The key outcome of this project has been the development of a number of tools – both mathematical and experimental – whereby the fundamental processes underlying geopolymerisation may be observed, analysed and quantified. The primary focus of this investigation has been to lay groundwork for future investigators rather than to select a single aspect of the geopolymerisation system and provide a complete analysis of it. That is not to say that the results of this investigation are by any means 'inconclusive' – but rather to highlight the fact that the fundamentally-based scientific investigation of geopolymers is a field that remains very much in its infancy.

The concept that zeolite formation may play a key role in determining the performance of geopolymers in certain applications, both in terms of the extent of crystallisation and the specific crystal structures produced, was developed. Based on a large body of evidence from the literature it was proposed that the X-ray amorphous geopolymer binder phase will, if formed under certain synthesis conditions or subjected to aggressive environments post-synthesis, contain (or develop) nanocrystalline zeolites. However, this proposal in itself is not the focus of the chapter – zeolite formation has been observed within geopolymers for over a decade, hence the format of the chapter as a literature review. However, the critical message from this part of the investigation is that, while zeolite formation has been previously observed, its importance has never before been stressed. In the tailored design of geopolymer formulations, it may be that the presence of crystallites is desirable in certain applications and undesirable in others. The work presented here provides a basis for future detailed analysis of the factors controlling crystallite development during (or following) geopolymerisation, with the possibility of, for example, tailoring crystallisation to maximise production of particular structures that selectively immobilise a given cation for radioactive or toxic waste immobilisation applications.

The model developed for Si/Al ordering within aluminosilicates also has applicability in analysis of geopolymer performance in immobilisation of (particularly cationic) wastes. By analysis of Si/Al ordering within the geopolymeric binder, the extent of framework cation disorder (and therefore Al-O-Al bond formation) was able to be calculated. Given the relatively

low strength and high reactivity of Al-O-Al bonds compared to Si-O-Al within an aluminosilicate framework, the ability to predict their extent of formation under certain synthesis conditions or in the presence of certain charge-balancing cations will be critical to the acceptance of geopolymers in applications where very long-term durability is required. When immobilisation on a geological timescale is required (e.g. in the case of long-half life radioactive materials), laboratory experimentation clearly cannot be conducted for a long enough period of time to obtain representative leaching data. Models for structural ordering within the gel matrix will therefore play a key role in the prediction of performance in these applications, as any simulations of leaching over a geological timescale will require an accurately-characterised system to use as an initial condition. The model and the ^{17}O 3QMAS-NMR data presented here provide such information, and is therefore expected to find application in development of geopolymer technology as a solution for some of the most pressing environmental contamination problems facing society in the 21st century.

The EDXRD technique provides a means of directly analysing the rates of dissolution of aluminosilicate source materials and the growth of new aluminosilicate phases. As was noted for the case of PDF analysis, the increasing worldwide availability of synchrotron radiation sources will allow more widespread use of this technique in future. While the results obtained here should be considered currently to be semiquantitative due to experimental limitations, future development and refinement of this technique, both in terms of experimental methodology and theoretical techniques for data analysis, will give further advances in this field. However, the results currently obtainable are quite sufficient for comparison with model predictions, and show trends matching those predicted from theory.

The reaction kinetic model described here ties together the rest of the investigation to provide a description of the full process of geopolymerisation from a somewhat empirical standpoint. By allowing the stoichiometry of all oligomeric and polymeric species to vary during reaction, the changes in Si/Al ratio in both the gel/solid and aqueous phases present during geopolymerisation are able to be modelled. The use of a limited silicate speciation model based on experimental data introduces the differing effects of different alkali metal cations into the model. The solid aluminosilicate sources are currently treated as being relatively homogeneous, and the effect of reactive contaminants is not considered. When the exact roles of contaminants and heterogeneous aluminosilicate sources have become better understood by further experimental investigation,

inclusion of these effects into a reaction kinetic model such as the one presented here will allow greater insight into the interplay between these and other factors influencing geopolymerisation.

In summary, the conclusion of this report is that the mathematical and theoretical description and analysis of geopolymerisation is a field in which very little work has previously been undertaken. By undertaking initial investigations in a number of wide-ranging yet related areas a basis has been provided for future work in this field, which is expected to be central to the widespread acceptance and utilisation of geopolymer technology in any of a number of key applications.

REFERENCES

Akolekar, D., Chaffee, A. and Howe, R. F. (1997). "The transformation of kaolin to low-silica X zeolite." Zeolites **19**(5-6): 359-365.

Alonso, S. and Palomo, A. (2001a). "Alkaline activation of metakaolin and calcium hydroxide mixtures: Influence of temperature, activator concentration and solids ratio." Materials Letters **47**(1-2): 55-62.

Alonso, S. and Palomo, A. (2001b). "Calorimetric study of alkaline activation of calcium hydroxide-metakaolin solid mixtures." Cement and Concrete Research **31**(1): 25-30.

Antonić, T. and Subotić, B. (1998). "Evidence of the "memory" effect of amorphous aluminosilicate gel precursors by simulation of zeolite crystallization processes using the population balance method." Croatica Chemica Acta **71**(4): 929-948.

Bao, Y., Kwan, S., Siemer, D. D. and Grutzeck, M. W. (2003). "Binders for radioactive waste forms made from pretreated calcined sodium bearing waste." Journal of Materials Science **39**(2): 481-488.

Barbosa, V. F. F., MacKenzie, K. J. D. and Thaumaturgo, C. (2000). "Synthesis and characterisation of materials based on inorganic polymers of alumina and silica: sodium polysialate polymers." International Journal of Inorganic Materials **2**(4): 309-317.

Barrer, R. M. and White, E. A. D. (1952). "The hydrothermal chemistry of silicates. Part II. Synthetic crystalline sodium aluminosilicates." Journal of the Chemical Society (5): 1561-1571.

Barrer, R. M. (1966). "Mineral synthesis by the hydrothermal technique." Chemistry in Britain **2**(9): 380-394.

Benharrats, N., Belbachir, M., Legrand, A. P. and D'Espinose de la Caillerie, J.-B. (2003). "^{29}Si and ^{27}Al MAS NMR study of the zeolitization of kaolin by alkali leaching." Clay Minerals **38**(1): 49-61.

Bosenick, A., Dove, M. T., Myers, E. R., Palin, E. J., Sainz-Diaz, C. I., Guiton, B. S., Warren, M. C., Craig, M. S. and Redfern, S. A. T. (2001). "Computational methods for the study of energies of cation distributions: Applications to cation-ordering phase transitions and solid solutions." Mineralogical Magazine **65**(2): 193-219.

Bursill, L. A., Lodge, E. A. and Thomas, J. M. (1980). "Zeolitic structures as revealed by high-resolution electron microscopy." Nature **286**(5769): 111-113.

Catlow, C. R. A., George, A. R. and Freeman, C. M. (1996). "Ab initio and molecular-mechanics studies of aluminosilicate fragments, and the origin of Lowenstein's rule." Chemical Communications (11): 1311-1312.

Cioffi, R., Maffucci, L. and Santoro, L. (2003). "Optimization of geopolymer synthesis by calcination and polycondensation of a kaolinitic residue." Resources, Conservation and Recycling **40**(1): 27-38.

Ciric, J. (1968). "Kinetics of zeolite A crystallization." Journal of Colloid and Interface Science **28**(2): 315-324.

Cournoyer, R. A., Kranich, W. L. and Sand, L. B. (1975). "Zeolite crystallisation kinetics related to dissolution rates of quartz reactant." Journal of Physical Chemistry **79**(15): 1578-1581.

Davidovits, J. (1988). Structural characterization of geopolymeric materials with X-ray diffractometry and MAS-NMR spectrometry. Proceedings of Geopolymer '88 - First European Conference on Soft Mineralurgy, Compeigne, France, Universite de Technologie de Compeigne, J. Davidovits and J. Orlinski, Eds, 149-166.

Davidovits, J. (1991). "Geopolymers - Inorganic polymeric new materials." Journal of Thermal Analysis **37**(8): 1633-1656.

Davis, M. E. and Lobo, R. F. (1992). "Zeolite and molecular sieve synthesis." Chemistry of Materials **4**(4): 756-768.

Dempsey, E., Kühl, G. H. and Olson, D. H. (1969). "Variation of lattice parameter with aluminum content in synthetic sodium faujasites. Evidence for ordering of framework ions." Journal of Physical Chemistry **73**(2): 387-390.

Diamond, S. (1986). "Particle morphologies in fly ash." Cement and Concrete Research **16**(4): 569-579.

Dutta, P. K., Shieh, D. C. and Puri, M. (1987). "Raman spectroscopic study of the synthesis of zeolite Y." Journal of Physical Chemistry **91**(9): 2332-2336.

Duxson, P., Provis, J. L., Lukey, G. C., Separovic, F. and van Deventer, J. S. J. (2005a). "^{29}Si NMR study of structural ordering in aluminosilicate geopolymer gels." Langmuir **21**(7): 3028-3036.

Duxson, P., Lukey, G. C., Separovic, F. and van Deventer, J. S. J. (2005b). "The effect of alkali cations on aluminum incorporation in geopolymeric gels." Industrial & Engineering Chemistry Research **44**(4): 832-839.

Duxson, P., Mallicoat, S. W., Lukey, G. C., Kriven, W. M. and van Deventer, J. S. J. (2006). "The effect of alkali and Si/Al ratio on the development of mechanical properties of metakaolin-based geopolymers." Colloids and Surfaces A - Physicochemical and Engineering Aspects **Submitted**.

Efstathiadis, H., Yin, Z. and Smith, F. W. (1992). "Atomic bonding in amorphous hydrogenated silicon carbide alloys: A statistical thermodynamic approach." Physical Review B **46**(20): 13119-13130.

Engelhardt, G., Hoebbel, D., Tarmak, M., Samoson, A. and Lippmaa, E. (1982). "^{29}Si-NMR-Untersuchungen zur Anionenstruktur von kristallinen Tetramethylammonium-alumosilicaten und -alumosilicatlösungen." Zeitschrift für Anorganische und Allgemeine Chemie **484**(1): 22-32.

Engelhardt, G. and Michel, D. (1987). High-Resolution Solid-State NMR of Silicates and Zeolites. Chichester, John Wiley & Sons, 485pp.

Faimon, J. (1996). "Oscillatory silicon and aluminum aqueous concentrations during experimental aluminosilicate weathering." Geochimica et Cosmochimica Acta **60**(15): 2901-2907.

Gabelica, Z., Nagy, J. B. and Debras, G. (1983). "Characterization of X-ray amorphous ZSM-5 zeolites by high resolution solid state ^{13}C-NMR spectroscopy." Journal of Catalysis **84**(1): 256-260.

Giessen, B. C. and Gordon, G. E. (1968). "X-ray diffraction: New high-speed technique based on X-ray spectrography." Science **159**(3818): 973-975.

Gordillo, M. C. and Herrero, C. P. (1992). "Temperature dependence of the Si,Al distribution in ultramarines." Chemical Physics Letters **200**(4): 424-428.

Gordon, M., Bell, J. L. and Kriven, W. M. (2004). "Comparison of naturally and synthetically derived, potassium-based geopolymers." Ceramic Transactions **165**: 95-106.

Granizo, M. L., Blanco-Varela, M. T. and Palomo, A. (2000). "Influence of the starting kaolin on alkali-activated materials based on metakaolin. Study of the reaction parameters by isothermal conduction calorimetry." Journal of Materials Science **35**(24): 6309-6315.

Granizo, M. L., Alonso, S., Blanco-Varela, M. T. and Palomo, A. (2002). "Alkaline activation of metakaolin: Effect of calcium hydroxide in the products of reaction." Journal of the American Ceramic Society **85**(1): 225-231.

Hass, E. C., Mezey, P. G. and Plath, P. J. (1982). "Non-empirical SCF molecular orbital studies on simple zeolite model systems." THEOCHEM - Journal of Molecular Structure **87**(3): 261-272.

Jacobs, P. A., Derouane, E. G. and Weitkamp, J. (1981). "Evidence for X-ray-amorphous zeolites." Journal of the Chemical Society - Chemical Communications (12): 591-593.

Kaps, C. and Buchwald, A. (2002). Property controlling influences on the generation of geopolymeric binders based on clay. Geopolymers 2002. Turn Potential into Profit., Melbourne, Siloxo Pty. Ltd., G. C. Lukey, Ed, CD-ROM Proceedings.

Klinowski, J., Thomas, J. M., Fyfe, C. A. and Hartman, J. S. (1982). "A re-examination of Si,Al ordering in zeolites Na-X and Na-Y." Journal of the Chemical Society - Faraday Transactions 2 **1982**(78): 1025-1050.

Klinowski, J. (1984). "Nuclear magnetic resonance studies of zeolites." Progress in Nuclear Magnetic Resonance Spectroscopy **16**(3-4): 237-309.

Kriven, W. M., Gordon, M. and Bell, J. L. (2004). "Geopolymers: Nanoparticulate, nanoporous ceramics made under ambient conditions." Microscopy and Microanalysis **10**(Supp. S02): 404-405.

Krivenko, P. V. and Kovalchuk, G. Y. (2002). Heat-resistant fly ash based geocements. Geopolymers 2002. Turn Potential into Profit., Melbourne, Australia, Siloxo Pty. Ltd., G. C. Lukey, Ed, CD-ROM Proceedings.

Lee, S. K. and Stebbins, J. F. (1999). "The degree of aluminum avoidance in aluminosilicate glasses." American Mineralogist **84**(5-6): 937-945.

Lee, S. K. and Stebbins, J. F. (2000). "Al-O-Al and Si-O-Si sites in framework aluminosilicate glasses with Si/Al=1: quantification of framework disorder." Journal of Non-Crystalline Solids **270**(1-3): 260-264.

Lee, W. K. W. and van Deventer, J. S. J. (2002). "The effect of ionic contaminants on the early-age properties of alkali-activated fly ash-based cements." Cement and Concrete Research **32**(4): 577-584.

Loewenstein, W. (1954). "The distribution of aluminum in the tetrahedra of silicates and aluminates." American Mineralogist **39**(1-2): 92-96.

Massiot, D., Touzo, B., Trumeau, D., Coutures, J. P., Virlet, J., Florian, P. and Grandinetti, P. J. (1996). "Two-dimensional magic-angle spinning isotropic reconstruction sequences for quadrupolar nuclei." Solid State Nuclear Magnetic Resonance **6**(1): 73-83.

Mintova, S., Olson, N. H. and Bein, T. (1999a). "Electron microscopy reveals the nucleation mechanism of zeolite Y from precursor colloids." Angewandte Chemie - International Edition **38**(21): 3201-3204.

Mintova, S., Olson, N. H., Valtchev, V. and Bein, T. (1999b). "Mechanism of zeolite A nanocrystal growth from colloids at room temperature." Science **283**(5404): 958-960.

Myers, E. R. (1999). "Al/Si ordering in silicate minerals." Ph.D. Thesis, Department of Earth Sciences, University of Cambridge, UK, 132pp.

Navrotsky, A. and Tian, Z.-R. (2001). "Systematics in the enthalpies of formation of anhydrous aluminosilicate zeolites, glasses, and dense phases." Chemistry - A European Journal **7**(4): 769-774.

Nguyen, M. H., Lee, S. J. and Kriven, W. M. (1999). "Synthesis of oxide powders by way of a polymeric steric entrapment precursor route." Journal of Materials Research **14**(8): 3417-3426.

Oelkers, E. H. and Gislason, S. R. (2001). "The mechanism, rates and consequences of basaltic glass dissolution: I. An experimental study of the dissolution rates of basaltic glass as a function of aqueous Al, Si and oxalic acid concentration at 25°C and pH = 3 and 11." Geochimica et Cosmochimica Acta **65**(21): 3671-3681.

Ogura, M., Kawazu, Y., Takahashi, H. and Okubo, T. (2003). "Aluminosilicate species in the hydrogel phase formed during the aging process for the crystallization of FAU zeolite." Chemistry of Materials **15**(13): 2661-2667.

Olanrewaju, J. (2002). "Hydrothermal transformation and dissolution of hydroceramic waste forms for the INEEL calcined high-level nuclear waste." Ph.D. Thesis, College of Earth and Mineral Sciences, Pennsylvania State University, 268pp.

Palin, E. J., Dove, M. T., Redfern, S. A. T., Bosenick, A., Sainz-Diaz, C. I. and Warren, M. C. (2001). "Computational study of tetrahedral Al-Si ordering in muscovite." Physics and Chemistry of Minerals **28**(8): 534-544.

Palomo, A. and Glasser, F. P. (1992). "Chemically-bonded cementitious materials based on metakaolin." British Ceramic Transactions and Journal **91**(4): 107-112.

Phair, J. W., van Deventer, J. S. J. and Smith, J. D. (2001). "Interaction of sodium silicate with zirconia and its consequences for polysialation." Colloids and Surfaces A - Physicochemical and Engineering Aspects **182**(1-3): 143-159.

Phillips, B. L., Kirkpatrick, R. J. and Carpenter, M. A. (1992). "Investigation of short-range Al,Si order in synthetic anorthite by ^{29}Si MAS NMR spectroscopy." American Mineralogist **77**(5-6): 484-494.

Provis, J. L., Duxson, P., Lukey, G. C. and van Deventer, J. S. J. (2005a). "A statistical thermodynamic model for Si/Al ordering in amorphous aluminosilicates." Chemistry of Materials **17**(11): 2976-2986.

Provis, J. L., Duxson, P., van Deventer, J. S. J. and Lukey, G. C. (2005b). "The role of mathematical modelling and gel chemistry in advancing geopolymer technology." Chemical Engineering Research & Design **83**(A7): 853-860.

Provis, J. L., Lukey, G. C. and van Deventer, J. S. J. (2005c). "Do geopolymers actually contain nanocrystalline zeolites? - A reexamination of existing results." Chemistry of Materials **17**(12): 3075-3085.

Provis, J. L., Duxson, P., Lukey, G. C., Separovic, F., Kriven, W. M. and van Deventer, J. S. J. (2005d). "Modeling speciation in highly concentrated alkaline silicate solutions." Industrial & Engineering Chemistry Research **44**(23): 8899-8908.

Provis, J. L. and van Deventer, J. S. J. (2006). "In-situ energy dispersive X-ray diffractometry - A direct measure of the kinetics of geopolymerisation." Journal of Materials Science **In Press Jan 06**.

Provis, J. L. (2006). "Modelling the Formation of Geopolymers." Ph.D. Thesis, Department of Chemical and Biomolecular Engineering, University of Melbourne.

Rahier, H., van Mele, B. and Wastiels, J. (1996a). "Low-temperature synthesized aluminosilicate glasses. 2. Rheological transformations during low-temperature cure and high-temperature properties of a model compound." Journal of Materials Science **31**(1): 80-85.

Rahier, H., van Mele, B., Biesemans, M., Wastiels, J. and Wu, X. (1996b). "Low-temperature synthesized aluminosilicate glasses. 1. Low-temperature reaction stoichiometry and structure of a model compound." Journal of Materials Science **31**(1): 71-79.

Rahier, H., Simons, W., van Mele, B. and Biesemans, M. (1997). "Low-temperature synthesized aluminosilicate glasses. 3. Influence of the composition of the silicate solution on production, structure and properties." Journal of Materials Science **32**(9): 2237-2247.

Rahier, H., Denayer, J. F. and van Mele, B. (2003). "Low-temperature synthesized aluminosilicate glasses. Part IV. Modulated DSC study on the effect of particle size of metakaolinite on the production of inorganic polymer glasses." Journal of Materials Science **38**(14): 3131-3136.

Ramdas, S., Thomas, J. M., Klinowski, J., Fyfe, C. A. and Hartman, J. S. (1981). "Ordering of aluminium and silicon in synthetic faujasites." Nature **292**(5820): 228-230.

Rocha, J., Klinowski, J. and Adams, J. M. (1991). "Synthesis of zeolite Na-A from metakaolinite revisited." Journal of the Chemical Society - Faraday Transactions **87**(18): 3091-3097.

Rowles, M. and O'Connor, B. (2003). "Chemical optimisation of the compressive strength of aluminosilicate geopolymers synthesised by sodium silicate activation of metakaolinite." Journal of Materials Chemistry **13**(5): 1161-1165.

Roy, D. (1999). "Alkali-activated cements - Opportunities and challenges." Cement and Concrete Research **29**(2): 249-254.

Šefčík, J. and McCormick, A. V. (1999). "Prediction of crystallization diagrams for synthesis of zeolites." Chemical Engineering Science **54**(15-16): 3513-3519.

Sindhunata (2006). "The Mechanisms and Kinetics of Fly Ash Based Geopolymerisation." Ph.D. Thesis, Department of Chemical and Biomolecular Engineering, University of Melbourne.

Subotić, B., Tonejc, A. M., Bagović, D., Čižmek, A. and Antonić, T. (1994). Electron diffraction and infrared spectroscopy of amorphous aluminosilicate gels. Zeolites and Related Microporous Materials: State of the Art 1994. J. Weitkamp, H. G. Karge, H. Pfeifer and W. Hölderich, Elsevier Science. **84A:** 259-266.

Tanaka, H., Miyagawa, A., Eguchi, H. and Hino, R. (2004). "Synthesis of a single-phase Na-A zeolite from coal fly ash by dialysis." Industrial & Engineering Chemistry Research **43**(19): 6090-6094.

van Jaarsveld, J. G. S., van Deventer, J. S. J. and Lorenzen, L. (1997). "The potential use of geopolymeric materials to immobilise toxic metals. 1. Theory and applications." Minerals Engineering **10**(7): 659-669.

van Jaarsveld, J. G. S. and van Deventer, J. S. J. (1999). "Effect of the alkali metal activator on the properties of fly ash-based geopolymers." Industrial & Engineering Chemistry Research **38**(10): 3932-3941.

van Jaarsveld, J. G. S. (2000). "The Physical and Chemical Characterisation of Fly Ash Based Geopolymers." Ph.D. Thesis, Department of Chemical Engineering, University of Melbourne, 381pp.

van Jaarsveld, J. G. S., van Deventer, J. S. J. and Lukey, G. C. (2003). "The characterisation of source materials in fly ash-based geopolymers." Materials Letters **57**(7): 1272-1280.

Vaughan, F. (1955). "Energy changes when kaolin minerals are heated." Clay Minerals Bulletin **2**(13): 265-274.

Wagman, D. D., Evans, W. H., Parker, V. B., Halow, I., Bailey, S. M. and Schumm, R. H. (1968). Selected Values of Chemical Thermodynamic Properties: Tables for the First Thirty-Four Elements in the Standard Order of Arrangement. Washington DC, U.S. Government Printing Office, 264pp.

Walther, J. V. (1996). "Relation between rates of aluminosilicate mineral dissolution, pH, temperature, and surface charge." American Journal of Science **296**(7): 693-728.

Walton, R. I., Millange, F., O'Hare, D., Davies, A. T., Sankar, G. and Catlow, C. R. A. (2001). "An in situ energy-dispersive X-ray diffraction study of the hydrothermal crystallization

of zeolite A. 1. Influence of reaction conditions and transformation into sodalite." Journal of Physical Chemistry B **105**(1): 83-90.

Wei, S., Zhang, Y.-S., Wei, L. and Liu, Z.-Y. (2004). "In situ monitoring of the hydration process of K-PS geopolymer cement with ESEM." Cement and Concrete Research **34**(6): 935-940.

Yang, H., Walton, R. I., Antonijevic, S., Wimperis, S. and Hannon, A. C. (2004). "Local order of amorphous zeolite precursors from $^{29}Si\{^{1}H\}$ CPMAS and ^{27}Al and ^{23}Na MQMAS NMR and evidence for the nature of medium-range order from neutron diffraction." Journal of Physical Chemistry B **108**(24): 8208-8217.

Yang, S., Navrotsky, A. and Phillips, B. L. (2000). "In situ calorimetric, structural, and compositional study of zeolite synthesis in the system $5.15Na_2O$-$1.00Al_2O_3$-$3.28SiO_2$-$165H_2O$." Journal of Physical Chemistry B **104**(25): 6071-6080.

Yip, C. K. and van Deventer, J. S. J. (2003). "Microanalysis of calcium silicate hydrate gel formed within a geopolymeric binder." Journal of Materials Science **38**(18): 3851-3860.

Yip, C. K., Lukey, G. C. and van Deventer, J. S. J. (2003). "Effect of blast furnace slag addition on microstructure and properties of metakaolinite geopolymeric materials." Ceramic Transactions **153**: 187-209.

PUBLICATIONS RELATED TO THIS PROJECT

JOURNAL PUBLICATIONS

(1) Provis, J. L.; van Deventer, J. S. J. "In-situ energy dispersive X-ray diffractometry - A direct measure of the kinetics of geopolymerisation." – Accepted for publication in a Special Edition of *Journal of Materials Science* on Geopolymer Science and Technology, Jan 2006.

(2) van Deventer, J. S. J.; Provis, J. L.; Duxson, P.; Lukey, G. C. "Reaction mechanisms in the geopolymeric conversion of inorganic waste to useful products." *Journal of Hazardous Materials*, accepted Dec 2005. (Presented as a keynote lecture, WasteEng 2005, Albi, France, May 2005)

(3) Provis, J. L.; Duxson, P.; Lukey, G. C.; van Deventer, J. S. J. "The role of mathematical modeling and gel chemistry in advancing geopolymer technology." *Transactions of the Institution of Chemical Engineers A: Chemical Engineering Research and Design*, **2005**, *83* (A7), 853-860. (presented at the 7th World Congress of Chemical Engineering, Glasgow, Scotland, July 2005)

(4) Provis, J. L.; Lukey, G. C.; van Deventer, J. S. J. "Are geopolymers largely composed of nanocrystalline zeolites? - A reexamination of existing results." *Chemistry of Materials*, **2005**, *17* (12), 3075-3085 – Featured as the cover article for *Chemistry of Materials*, Vol. 17, Iss. 12.

(5) Provis, J. L.; Duxson, P.; Lukey, G. C.; van Deventer, J. S. J. "A statistical thermodynamic model for Si/Al ordering in amorphous aluminosilicates." *Chemistry of Materials*, **2005,** *17* (11), 2976-2986.

(6) Duxson, P.; Provis, J. L.; Lukey, G. C.; Separovic, F.; van Deventer, J. S. J. "^{29}Si MAS NMR investigation of structural ordering in aluminosilicate geopolymer gels." *Langmuir*, **2005,** *21* (7), 3028-3036.

CONFERENCE PUBLICATIONS

(1) van Deventer, J. S. J.; Provis, J. L.; Duxson, P.; Lukey, G. C. "Technological, environmental and commercial drivers for the use of geopolymers in a sustainable materials industry"; 2006 TMS Fall Extraction & Processing Meeting: Sohn International Symposium, San Diego, CA, 27-31 Aug 2006 – to be published in a forthcoming TMS Proceedings volume.

(2) van Deventer, J. S. J.; Duxson, P.; Provis, J. L.; Lukey, G. C. "Recent progress in the development of geopolymer cements"; International Forum on Waste Utilization in Cement and Concrete Industries, Beijing, China, 27-28 March 2006 – to be published in a Proceedings volume by China Building Materials Association, Y.-S. Cui, Ed.

(3) Duxson, P., Provis, J. L.; Lukey, G. C.; van Deventer, J. S. J. "The characterization of nanostructure and structural ordering in aluminosilicate geopolymer gels"; Geopolymers 2005, Saint-Quentin, France, July 2005, CD-ROM Proceedings.

(4) van Deventer, J. S. J.; Lukey, G. C.; Provis, J. L. "The role of geopolymerisation in sustainable minerals processing"; John Floyd International Symposium, Melbourne, Australia, July 2005, CD-ROM Proceedings.

(5) Provis, J. L.; Duxson, P.; Lukey, G. C.; van Deventer, J. S. J. "Modelling chemical ordering in aluminosilicates and subsequent prediction of cation immobilisation efficiency"; WasteEng 2005, Albi, France, May 2005, CD-ROM Proceedings.

(6) Provis, J. L.; Duxson, P.; Lukey, G. C.; van Deventer, J. S. J. "Modeling Si/Al ordering in metakaolin-based geopolymers"; 107th Annual Meeting and Exposition of the American Ceramic Society, Baltimore, MD, April 2005 – To be published in *Ceramic Transactions*, **2006**, *175*.

OTHER CONFERENCE PRESENTATIONS

(1) Provis, J. L., Duxson, P., Lukey, G. C. and van Deventer, J. S. J. "Modeling geopolymer formation"; Novel and Emerging Ceramics and Composites, Kona, HI, 25-30 Jun 2006.

(2) Duxson, P.; Provis, J. L.; Lukey, G. C.; van Deventer, J. S. J. "Geopolymers: A multinuclear SS NMR investigation of structural ordering"; 1st Asia-Pacific NMR Symposium, Yokohama, Japan, Nov 2005.